

## Long-range additive and nonadditive potentials in a hybrid system: Ground-state atom, excited-state atom, and ion

Pei-Gen Yan <sup>1</sup>, Li-Yan Tang <sup>2,\*</sup>, Zong-Chao Yan,<sup>1,2</sup> and James F. Babb <sup>3,†</sup>

<sup>1</sup>*Department of Physics, University of New Brunswick, Fredericton, New Brunswick, Canada E3B 5A3*

<sup>2</sup>*State Key Laboratory of Magnetic Resonance and Atomic and Molecular Physics, Wuhan Institute of Physics and Mathematics, Innovation Academy for Precision Measurement Science and Technology, Chinese Academy of Sciences, Wuhan 430071, People's Republic of China*

<sup>3</sup>*ITAMP, Center for Astrophysics|Harvard & Smithsonian, 60 Garden Street, Cambridge, Massachusetts 02138, USA*



(Received 23 March 2021; revised 28 June 2021; accepted 22 July 2021; published 10 August 2021)

We report a theoretical study on the long-range additive and nonadditive potentials for a three-body hybrid atom-atom-ion system composed of one ground-*S*-state Li atom, one excited-*P*-state Li atom, and one ground-*S*-state Li<sup>+</sup> ion, Li( $2^2S$ )-Li( $2^2P$ )-Li<sup>+</sup>( $1^1S$ ). The interaction coefficients are evaluated with highly accurate wave functions calculated variationally in Hylleraas coordinates. For this hybrid system the three-body nonadditive interactions (appearing in second order) induced by the energy degeneracy and enhanced by the induction effect of the Li<sup>+</sup> ion through the internal electric field can be strong and even stronger than the two-body additive interactions at the same order. We find that for particular geometries the two-body additive interactions of the system sum to zero, leaving only three-body nonadditive interactions, thus making the present system potentially a platform to explore quantum three-body effects. We also extract by first principles the leading coefficients of the long-range electrostatic, induction, and dispersion energies of Li<sub>2</sub><sup>+</sup> electronic states correlating to Li<sup>+</sup>( $1^1S$ )-Li( $2^2P$ ). The results should be especially valuable for the exploration of schemes to create trimers with ultracold atoms and ions in optical lattices.

DOI: [10.1103/PhysRevA.104.022807](https://doi.org/10.1103/PhysRevA.104.022807)

### I. INTRODUCTION

This paper provides detailed results for the long-range interactions between three atomic systems, specifically, a ground-state atom, a (low-lying) excited-state atom, and a ground-state ion, for the particular case of lithium, specifically, Li( $2^2S$ )-Li( $2^2P$ )-Li<sup>+</sup>( $1^1S$ ). Most studies of hybrid systems consisting of ground- or low-lying-state atoms have been concerned with pairwise cases, i.e., an atom and an ion (reviewed in Ref. [1]) or a diatomic molecule and an ion [2–4]. Recently, properties of low-lying states of triatomic cations were systematically studied [5]. Also, some studies, while considering excitation of atoms, do not consider ions. For three atoms, with at least one atom in a Rydberg state, there are a number of studies, such as Refs. [6,7]. Other studies have considered three-body interactions of diatomic molecules in a trapping potential [8,9].

We explore another possibility: three atomic systems that are in the long-range domain (sufficiently separated such that electron exchange is small) with one constituent charged and one constituent *electronically excited*. There are two main results. First, we give expressions for the long-range potentials as expansions in inverse powers of separation distances and corresponding precisely evaluated coefficients for two-body

(dipole-dipole and van der Waals) and three-body (van der Waals) long-range additive and nonadditive interactions, in a manner similar to but extending our previous work on three atoms [10,11] and on two atoms and a ground state ion [12]. While in the present work the derived formulas are generally applicable to the hybrid  $A(n_0S)$ - $A(n'_0L)$ - $A^{Q+}(n''_0S)$  systems, even involving Rydberg states, we choose the particular states of lithium because we can evaluate the coefficients precisely using accurate wave functions. We discuss applications for quantum chemical studies of Li<sub>3</sub><sup>+</sup> and, as a consequence of our formulation, for long-range potential energies of Li<sub>2</sub><sup>+</sup> electronic states correlating to Li<sup>+</sup>( $1^1S$ )-Li( $2^2P$ ). Second, different from previous studies on the weak nonadditive interactions for three-body systems composed of atoms [10,11,13–19] or of two atoms and an ion [12], here we find theoretical evidence of a new pure quantum three-body effect that might have influence on constructing accurate potential surfaces. Specifically, for the Li( $2^2S$ )-Li( $2^2P$ )-Li<sup>+</sup>( $1^1S$ ) system, we find that at particular geometries the two-body additive interactions disappear, leaving only three-body nonadditive interactions. These net effects of two- and three-body interactions are quite similar to those for two- and three-body interactions in the case of polar molecules confined in lattice traps [8,9] or three Rydberg atoms under the influence of an external electric field [7], where the same goal, removal of two-body interactions, was pursued. To provide necessary context, we begin with some general contextual background from molecular (chemical) physics and from ultracold science.

\*lytang@wipm.ac.cn

†jbabb@cfa.harvard.edu

### A. General aspects of triatomic systems

The intrinsic complexity of triatomic molecules<sup>1</sup> produces interesting phenomena such as conical intersections and geometric phases [23,24] and the Renner-Teller effect [25], while consideration of three atoms at ultralow energies leads to Efimov [26,27], Borromean [9], and Pfaffian [8,28] states and makes the description of collisional processes such as atom-diatom collisions [29,30] and three-body recombination loss [31–33] challenging. The demands for understanding the spectroscopy and collisional processes of specific important triatomic molecules at thermal collisional energies also continue to drive progress. For example, ozone (O<sub>3</sub>) is a vital atmospheric constituent of the planet, with quantum-mechanical collisional cross sections recently reported (see Ref. [34] and references therein), tricarbon (C<sub>3</sub>) is prominent in comets and other astrophysical [35] and laboratory realms [36], and H<sub>3</sub>, H<sub>3</sub><sup>+</sup>, and their isotopologues serve as long-standing theoretical benchmark systems [23,37] and are important in astrophysical applications such as the cooling of hydrogen gas in molecular clouds [38] and the evolution of the early universe [39].

Detailed procedures for calculating and constructing potential energy surfaces (and other properties) of triatomic systems have been developed, as exemplified (for the representative molecules discussed above) by recent works such as for tricarbon [40], for ozone [41–43], and for H<sub>3</sub> [44]. A successful strategy to construct three-atom potential energy surfaces using semiempirical methods requires input calculations of atom-dimer and three-atom long-range potentials [45–47]. To understand the dynamics of low-energy (ultra-cold) collisions, consideration of the long-range potentials is paramount; see, for example, [2,3,48–50] for atom-molecule systems and [51–53] for atom-molecular-ion systems. Next we provide an overview of the lithium dimer and trimer cations.

### B. Homonuclear lithium dimer and trimer cations: Excited electronic states

We provide a brief overview of relevant work on the lithium homonuclear systems Li<sub>2</sub><sup>+</sup> and Li<sub>3</sub><sup>+</sup> in order to demonstrate the contrast between the data provided by the present work and those available in the literature.

For the diatomic lithium cation Li<sub>2</sub><sup>+</sup>, four electronic states (ignoring fine structure) correlate to the separated pair Li<sup>+</sup>(1<sup>1</sup>S)-Li(2<sup>2</sup>P), namely, 2<sup>2</sup>Σ<sub>g</sub>, 2<sup>2</sup>Σ<sub>u</sub>, 1<sup>2</sup>Π<sub>g</sub>, and 1<sup>2</sup>Π<sub>u</sub>. Model potential method calculations were given by Magnier *et al.* [54] and by Rabli and McCarroll [55]; a complete active space self-consistent field, multireference configuration-interaction calculation was reported in Ref. [56] (see also references therein for earlier work). Magnier *et al.* [54] calculated long-range potential curves as functions of

<sup>1</sup>A widely known aphorism, attributed to Schawlow, warns atomic physicists that “a diatomic molecule is one atom too many” [20], but it may be predated by an earlier observation attributed to Herschbach: “The trouble with triatomic molecules is, they have one atom too many!” [21]. Recently, Gao [22] emphasized the emergence of chemical complexity beginning with three atoms.

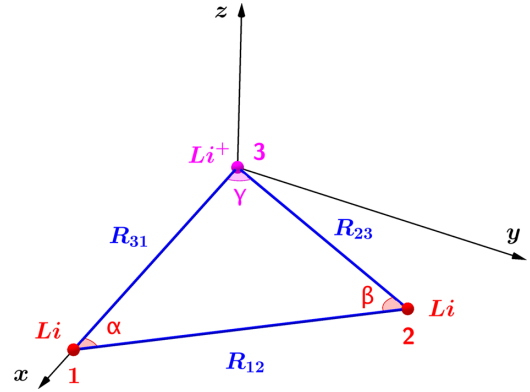


FIG. 1. Configuration of the Li(2<sup>2</sup>S)-Li(2<sup>2</sup>P)-Li<sup>+</sup>(1<sup>1</sup>S) system. The three particles define the *x-y* plane with the two neutral atoms labeled 1 and 2 and the ion labeled 3, the  $R_{IJ}$  are the internuclear distances, and  $\alpha$ ,  $\beta$ , and  $\gamma$  are the interior angles.

internuclear distance  $R$ , including the exchange energies and electrostatic, induction, and dispersion terms up to  $O(R^{-8})$ , but did not give the long-range potential coefficients. The emphasis of the present paper is on the three-body system, but because the two-body interactions are available from our calculations, as will be shown in Secs. II G–III, we will extract the values of the long-range potential coefficients of the four states of Li<sub>2</sub><sup>+</sup>.

For the triatomic lithium cation Li<sub>3</sub><sup>+</sup>, because we have found no previous quantum chemical studies of the excited electronic states corresponding to those reported here, we present a summary of calculations on the ground electronic state of Li<sub>3</sub><sup>+</sup>. In a series of works, Dunne and co-workers [57–60] calculated the ground-state potential energy and dipole moment surfaces, which were utilized to calculate rovibrational spectra [61,62]. Surprisingly, we have found few subsequent studies on the Li<sub>3</sub><sup>+</sup> ground electronic state [63], although very recently, as part of a systematic study exploring alkali-metal and alkaline-earth-metal hybrid ion-atom diatomic and triatomic systems, Śmiałkowski and Tomza [5] calculated equilibrium properties of the ground <sup>1</sup>A<sub>1</sub> and lowest triplet <sup>3</sup>B<sub>2</sub> states of Li<sub>3</sub><sup>+</sup>. Our previous paper [12] supplies the long-range interactions for the ground and lowest triplet states of Li<sub>3</sub><sup>+</sup>. In advance of awaited *ab initio* quantum chemical calculations, in the present work we calculate the long-range interaction potentials of Li<sub>3</sub><sup>+</sup> when one Li atom is Li(2<sup>2</sup>P).

### C. Similarity to lattice studies

Büchler *et al.* derived a Hubbard model for cold polar molecules trapped in an optical lattice [64], with the intent of realizing a system that could be used to model Hamiltonians that exhibit exotic ground-state properties [8,9]. In terms of the intermolecular interactions within the lattice, they write

$$U_{ij} = U_0 a^3 |\mathbf{R}_i - \mathbf{R}_j|^{-3} + U_1 a^6 |\mathbf{R}_i - \mathbf{R}_j|^{-6} \quad (1)$$

and

$$W_{ijk} = W_0 a^6 |\mathbf{R}_i - \mathbf{R}_j|^{-3} |\mathbf{R}_i - \mathbf{R}_k|^{-3}, \quad (2)$$

where  $U_0$ ,  $U_1$ , and  $W_0$  are certain energy scales;  $a$  is a length scale;  $i$ ,  $j$ , and  $k$  label the particles; the indices  $i$ ,  $j$ , and  $k$

are cyclically permuted; and  $\mathbf{R}_i$  are certain position vectors of the lattice site (see Ref. [64] for the complete definitions). By appropriate dressing of the cold molecules by an external static electric field and a microwave field, they show that the two-body interactions may be tuned “from repulsive to attractive, and even switched off, while the three-body terms remain repulsive and strong.” We will derive two equations for the present system, Eqs. (21) and (33), respectively, that are of the same form, but with additional terms, as Eqs. (1) and (2). We will show that at specific geometries we recover exactly Eqs. (1) and (2). The anisotropies of the interactions in the present system due to the ion charge and the excited  $\text{Li}(2^2P)$  atom are similar to the anisotropies due to the intermolecular dipole-dipole interactions in the optical-lattice-trapped cold polar molecular system [65–68]. Further discussion will be given in Sec. III E.

## II. THEORETICAL FORMULATION

The geometry of the three-body system is shown in Fig. 1, in which the three particles define a plane with the two neutral

atoms labeled as 1 and 2 and the ion labeled as 3. It is important to note that due to the degeneracy of atoms 1 and 2 we cannot specify which one is in the ground state or excited state. The interior angles of the configuration are  $\alpha$ ,  $\beta$ , and  $\gamma$ .

### A. Coulomb potential expansion

In the present work we take the electrostatic interaction  $V_{123}$  between pairs of particles for the  $\text{Li}(n_0 S)\text{-Li}(n_0 L)\text{-Li}^+(n'_0 S)$  system as a perturbation,

$$V_{123} = V_{12} + V_{23} + V_{31}, \quad (3)$$

where  $V_{12}$ ,  $V_{23}$ , and  $V_{31}$  are the two-body mutual electrostatic interactions between atoms 1 and 2 and ion 3. For three well-separated atoms or ions, the mutual interaction energy  $V_{IJ}$  can be expanded with the same method as used in Refs. [10–12]; thus,

$$V_{IJ} = \sum_{l_I l_J} \sum_{m_I m_J} T_{l_I - m_I}(\boldsymbol{\sigma}) T_{l_J m_J}(\boldsymbol{\rho}) W_{l_I l_J}^{m_I - m_J}(IJ), \quad (4)$$

where the geometry factor is

$$W_{l_I l_J}^{m_I - m_J}(IJ) = \frac{4\pi(-1)^{l_I}}{R_{IJ}^{l_I + l_J + 1}} \frac{(l_I + l_J - m_I + m_J)!(l_I, l_J)^{-1/2}}{[(l_I + m_I)!(l_I - m_I)!(l_J + m_J)!(l_J - m_J)!]^{1/2}} P_{l_I + l_J}^{m_I - m_J}(\cos \theta_{IJ}) \exp[i(m_I - m_J)\Phi_{IJ}], \quad (5)$$

where  $\mathbf{R}_{IJ} = \mathbf{R}_J - \mathbf{R}_I$  is the relative position vector from particle  $I$  to particle  $J$ , the notation  $(l_I, l_J, \dots) = (2l_I + 1)(2l_J + 1)\dots$ , and  $P_{l_I + l_J}^{m_I - m_J}(\cos \theta_{IJ})$  is the associated Legendre function with  $\theta_{IJ}$  representing the angle between  $\mathbf{R}_{IJ}$  and the  $z$  axis. The  $2^\ell$ -pole transition operator of an atom consisting of  $n + 1$  charged particles in the laboratory frame is defined as in Ref. [69],

$$T_{\ell m}(\rho) = \sum_{i=0}^n q_i \rho_i^\ell Y_{\ell m}(\hat{\rho}_i), \quad (6)$$

where  $q_i$  is the charge of the  $i$ th subparticle of the atom. In the center-of-mass frame [69],  $\rho_i$  becomes

$$\rho_i = \sum_{j=1}^n \epsilon_{ij} \mathbf{r}_j, \quad (7)$$

where  $\mathbf{r}_i = \rho_i - \rho_0$ ,  $\epsilon_{ij} = \delta_{ij} - m_j/M_T$ ,  $i = 0, 1, 2, \dots, n$ ,  $j = 1, 2, \dots, n$ , and  $M_T$  represents the total mass of the system. Using the formula

$$Y_{\ell m}(\hat{\mathbf{r}}) = \sqrt{\frac{3}{4\pi}} \prod_{i=1}^{\ell-1} \left( \sqrt{\frac{2i+3}{i+1}} \right) \underbrace{(\hat{\mathbf{r}} \otimes \hat{\mathbf{r}} \otimes \dots \otimes \hat{\mathbf{r}})_m^{(\ell)}}_{\ell}, \quad (8)$$

where  $\otimes$  denotes the coupling between two irreducible tensor operators, the  $2^\ell$ -pole transition operator can be simplified as

$$T_\ell = \sqrt{\frac{3}{4\pi}} \prod_{m=1}^{\ell-1} \left( \sqrt{\frac{2m+3}{m+1}} \right) \sum_{j_1, \dots, j_\ell} \left( \sum_{i=0}^n q_i \epsilon_{ij_1} \epsilon_{ij_2} \dots \epsilon_{ij_\ell} \right) \underbrace{(\hat{\mathbf{r}}_{j_1} \otimes \hat{\mathbf{r}}_{j_2} \otimes \dots \otimes \hat{\mathbf{r}}_{j_\ell})_0^{(\ell)}}_{\ell}. \quad (9)$$

For a four-body system, the explicit forms of transition operators  $T_\ell$  with  $\ell$  up to 3 can be found in Ref. [70].

### B. Hylleraas basis set

The nonrelativistic Hamiltonian of the Li atom in the center-of-mass frame [71] can be written as

$$H = -\frac{1}{2\mu} \sum_{i=1}^3 \nabla_i^2 - \frac{1}{m_0} \sum_{i>j \geq 1}^3 \nabla_i \cdot \nabla_j + q_0 \sum_{i=1}^3 \frac{q_i}{r_i} + \sum_{i>j \geq 1}^3 \frac{q_i q_j}{r_{ij}}, \quad (10)$$

where  $\mu = m_e m_0 / (m_e + m_0)$  is the reduced mass between an electron  $m_e$  and the nucleus  $m_0$ . The basis set is constructed in Hylleraas coordinates

$$\phi(\mathbf{r}_1, \mathbf{r}_2, \mathbf{r}_3) = r_1^{j_1} r_2^{j_2} r_3^{j_3} r_{12}^{j_{12}} r_{23}^{j_{23}} r_{31}^{j_{31}} e^{-\alpha r_1 - \beta r_2 - \gamma r_3} \mathcal{Y}_{(\ell_1 \ell_2) \ell_{12}, \ell_3}^{(LM)}(\hat{\mathbf{r}}_1, \hat{\mathbf{r}}_2, \hat{\mathbf{r}}_3) \mathcal{X}(1, 2, 3), \quad (11)$$

where

$$\mathcal{Y}_{(\ell_1 \ell_2 \ell_{12}, \ell_3)}^{(LM)}(\hat{\mathbf{r}}_1, \hat{\mathbf{r}}_2, \hat{\mathbf{r}}_3) = \sum_{m_i} \langle \ell_1 m_1; \ell_2 m_2 | \ell_{12} m_{12} \rangle \langle \ell_{12} m_{12}; \ell_3 m_3 | \ell_{12} \ell_3; LM_L \rangle Y_{\ell_1 m_1}(\hat{\mathbf{r}}_1) Y_{\ell_2 m_2}(\hat{\mathbf{r}}_2) Y_{\ell_3 m_3}(\hat{\mathbf{r}}_3) \quad (12)$$

is a vector-coupled product of spherical harmonics to form an eigenstate of the total angular momentum  $L$  and component  $M_L$ , and  $\mathcal{X}(1, 2, 3)$  is the three-electron spin- $\frac{1}{2}$  function. The variational wave function of the Li atom is a linear combination of basis functions  $\phi$  antisymmetrized. With some truncations to avoid the numerical linear dependence, all terms in Eq. (11) are included such that

$$j_1 + j_2 + j_3 + j_{12} + j_{23} + j_{31} \leq \Omega, \quad (13)$$

where  $\Omega$  is an integer, and the convergence for the energy eigenvalue is studied by increasing  $\Omega$  progressively. The reduced matrix elements for various transition operators can be evaluated with the basic integral

$$\int d\mathbf{r}_1 d\mathbf{r}_2 d\mathbf{r}_3 r_1^{j_1} r_2^{j_2} r_3^{j_3} r_{12}^{j_{12}} r_{23}^{j_{23}} r_{31}^{j_{31}} e^{-\alpha r_1 - \beta r_2 - \gamma r_3} \times Y_{\ell'_1 m'_1}^*(\mathbf{r}_1) Y_{\ell'_2 m'_2}^*(\mathbf{r}_2) Y_{\ell'_3 m'_3}^*(\mathbf{r}_3) Y_{\ell_1 m_1}(\mathbf{r}_1) Y_{\ell_2 m_2}(\mathbf{r}_2) Y_{\ell_3 m_3}(\mathbf{r}_3). \quad (14)$$

The details of the computational method for this integral are developed in Refs. [71,72]. Similarly, for the  $\text{Li}^+$  ion, we also use the Hylleraas variational method to obtain the energies, wave functions, and transition matrix elements. The detailed Hylleraas method for a two-electron atom is given in Ref. [73].

### C. Zeroth-order wave function

For the degenerate  $\text{Li}(n_0S)\text{-Li}(n_0L)\text{-Li}^+(n'_0S)$  system with energy  $E_{n_0 n_0 n'_0}^{(0)} = E_{n_0 S}^{(0)} + E_{n_0 L}^{(0)} + E_{n'_0 S}^{(0)}$ , the zeroth-order wave function can be written as

$$|\Psi^{(0)}\rangle = a|n_0L; n_00; n'_00\rangle + b|n_00; n_0L; n'_00\rangle, \quad (15)$$

where  $a$  and  $b$  are the expansion coefficients of the zeroth-order wave function in the basis set  $\{|n_0L; n_00; n'_00\rangle, |n_00; n_0L; n'_00\rangle\}$ , with  $|n_00\rangle$ ,  $|n_0L\rangle$ , and  $|n'_00\rangle$  the initial states for  $\text{Li}(n_0S)$ ,  $\text{Li}(n_0L)$ , and  $\text{Li}^+(n_0S)$ , respectively. The corresponding zeroth-order wave functions (or the values of  $a$  and  $b$ ) depend on the geometrical configuration formed by the three particles and are determined by diagonalizing the perturbation in this basis set. Then using the degenerate perturbation theory, we can obtain the long-range part of the interaction potential for the  $\text{Li}(2^2S)\text{-Li}(2^2P)\text{-Li}^+(1^1S)$  system, which can be written as

$$\Delta E = \Delta E_{\text{add}}^{(1)} + \Delta E_{\text{add}}^{(2)} + \Delta E_{\text{non}}^{(2)}, \quad (16)$$

where  $\Delta E_{\text{add}}^{(1)}$  and  $\Delta E_{\text{add}}^{(2)}$  are the first-order and second-order additive interactions, respectively, and  $\Delta E_{\text{non}}^{(2)}$  is the second-order nonadditive interaction.

### D. First-order additive interactions

The first-order additive interaction  $\Delta E_{\text{add}}^{(1)}$  is given by

$$\Delta E_{\text{add}}^{(1)} = -\frac{C_3^{(12)}(1, M)}{R_{12}^3} - \frac{C_3^{(23)}(1, M)}{R_{23}^3} - \frac{C_3^{(31)}(1, M)}{R_{31}^3}, \quad (17)$$

where  $C_3^{(12)}(1, M)$  describes the dipole-dipole interaction between two neutral atoms. In addition,  $C_3^{(23)}(1, M)$  and  $C_3^{(31)}(1, M)$  describe the electrostatic interaction between the charge of the ion labeled as 3 and the quadrupole moments of atom 2 and atom 1, respectively; the quadrupole moment comes from the excited  $\text{Li}(2^2P)$  atom, which can be atom 1 or atom 2 due to the degeneracy of the three-body system. These leading long-range interaction coefficients are given by

$$C_3^{(12)}(1, M) = (a^*b + b^*a) \frac{4\pi(-1)^{1+M}}{9(1-M)!(1+M)!} |\langle n_00 \| T_1 \| n_01 \rangle|^2, \quad (18)$$

$$C_3^{(23)}(1, M) = |b|^2 Q(-1)^{1+M} \sqrt{\frac{\pi}{5}} \begin{pmatrix} 1 & 2 & 1 \\ -M & 0 & M \end{pmatrix} \langle n_01 \| T_2 \| n_01 \rangle, \quad (19)$$

$$C_3^{(31)}(1, M) = |a|^2 Q(-1)^{1+M} \sqrt{\frac{\pi}{5}} \begin{pmatrix} 1 & 2 & 1 \\ -M & 0 & M \end{pmatrix} \langle n_01 \| T_2 \| n_01 \rangle, \quad (20)$$

where  $Q$  is the charge of the ion,  $M$  represents the magnetic quantum number of the excited  $\text{Li}(2^2P)$  atom, and  $T_\ell$  is the  $2^\ell$ -pole transition operator, which is defined in Sec. II A.

### E. Second-order additive interactions

The second-order additive interaction  $\Delta E_{\text{add}}^{(2)}$  is given by

$$\Delta E_{\text{add}}^{(2)} = -\frac{C_4^{(23)}(1, M)}{R_{23}^4} - \frac{C_4^{(31)}(1, M)}{R_{31}^4} - \frac{C_6^{(12)}(1, M)}{R_{12}^6} - \frac{C_6^{(23)}(1, M)}{R_{23}^6} - \frac{C_6^{(31)}(1, M)}{R_{31}^6} - \dots, \quad (21)$$

where  $C_4^{(23)}(1, M)$  and  $C_4^{(31)}(1, M)$  describe the induction interactions between ion 3 and neutral atoms 2 and 1, respectively. The dispersion interaction coefficient between the neutral atoms 1 and 2 is given by  $C_6^{(12)}(1, M)$ , while  $C_6^{(23)}(1, M)$  and  $C_6^{(31)}(1, M)$  describe the interactions between ion 3 and the two neutral atoms 2 and 1, respectively, including both the induction and the dispersion interaction coefficients. The corresponding expressions for the additive coefficients are

$$C_4^{(23)}(1, M) = |a|^2 \mathbb{T}_1 + |b|^2 \mathbb{T}_3(M), \quad (22)$$

$$C_4^{(31)}(1, M) = |a|^2 \mathbb{T}_3(M) + |b|^2 \mathbb{T}_1, \quad (23)$$

$$C_6^{(23)}(1, M) = |a|^2 \mathbb{T}_2 + |b|^2 \mathbb{T}_5(M), \quad (25)$$

$$C_6^{(12)}(1, M) = |a|^2 \mathbb{T}_4(M) + |b|^2 \mathbb{T}_4(M), \quad (24)$$

$$C_6^{(31)}(1, M) = |a|^2 \mathbb{T}_5(M) + |b|^2 \mathbb{T}_2, \quad (26)$$

where

$$\mathbb{T}_1 = \frac{4\pi Q^2}{9} \sum'_{n_t} \frac{|\langle n_0 0 \| T_1 \| n_t 1 \rangle|^2}{E_{n_t 1} - E_{n_0 0}^{(0)}}, \quad (27)$$

$$\mathbb{T}_2 = \frac{4\pi Q^2}{25} \sum'_{n_t} \frac{|\langle n_0 0 \| T_2 \| n_t 2 \rangle|^2}{E_{n_t 2} - E_{n_0 0}^{(0)}} + \frac{32\pi^2}{27} \sum'_{n_t n_u} \frac{|\langle n_0 0 \| T_1 \| n_t 1 \rangle|^2 |\langle n_0 0 \| T_1 \| n_u 1 \rangle|^2}{(E_{n_t 1} - E_{n_0 0}^{(0)}) + (E_{n_u 1} - E_{n_0 0}^{(0)})}, \quad (28)$$

$$\mathbb{T}_3(M) = \frac{Q^2}{4\pi} \sum'_{n_t L_t} \frac{G_1(L_t, 0; 1, 1; 1, M) |\langle n_0 1 \| T_1 \| n_t L_t \rangle|^2}{E_{n_t L_t} - E_{n_0 1}^{(0)}}, \quad (29)$$

$$\mathbb{T}_4(M) = \sum'_{n_t n_u L_t} \frac{G_1(L_t, 1; 1, 1; 1, M) |\langle n_0 1 \| T_1 \| n_t L_t \rangle|^2 |\langle n_0 0 \| T_1 \| n_u 1 \rangle|^2}{(E_{n_t L_t} - E_{n_0 1}^{(0)}) + (E_{n_u 1} - E_{n_0 0}^{(0)})}, \quad (30)$$

$$\begin{aligned} \mathbb{T}_5(M) = & \sum'_{n_t n_u L_t} \frac{G_1(L_t, 1; 1, 1; 1, M) |\langle n_0 1 \| T_1 \| n_t L_t \rangle|^2 |\langle n_0 0 \| T_1 \| n_u 1 \rangle|^2}{(E_{n_t L_t} - E_{n_0 1}^{(0)}) + (E_{n_u 1} - E_{n_0 0}^{(0)})} + \frac{Q^2}{4\pi} \sum'_{n_t L_t} \left\{ \frac{G_1(L_t, 0; 2, 2; 1, M) |\langle n_0 1 \| T_2 \| n_t L_t \rangle|^2}{E_{n_t L_t} - E_{n_0 1}^{(0)}} \right. \\ & \left. + \frac{G_1(L_t, 0; 1, 3; 1, M) \langle n_0 1 \| T_1 \| n_t L_t \rangle^* \langle n_0 1 \| T_3 \| n_t L_t \rangle}{E_{n_t L_t} - E_{n_0 1}^{(0)}} + \frac{G_1(L_t, 0; 3, 1; 1, M) \langle n_0 1 \| T_3 \| n_t L_t \rangle^* \langle n_0 1 \| T_1 \| n_t L_t \rangle}{E_{n_t L_t} - E_{n_0 1}^{(0)}} \right\}, \quad (31) \end{aligned}$$

with the  $G_1$  function defined by

$$\begin{aligned} G_1(L_i, L_j; \ell_k, \ell'_k; L, M) = & \frac{16\pi^2 (\ell_k, \ell'_k)^{-1/2}}{(2L_j + 1)^2} \sum_{M_i, M_j, m_k} \begin{pmatrix} L & \ell_k & L_i \\ -M & m_k & M_i \end{pmatrix} \begin{pmatrix} L & \ell'_k & L_i \\ -M & m_k & M_i \end{pmatrix} \\ & \times \frac{(L_j + \ell_k - M_j + m_k)! (L_j + \ell'_k - M_j + m_k)! P_{L_j + \ell_k}^{M_j - m_k}(0) P_{L_j + \ell'_k}^{M_j - m_k}(0)}{(L_j + M_j)! (L_j - M_j)! (\ell_k + m_k)! (\ell_k - m_k)! (\ell'_k + m_k)! (\ell'_k - m_k)!^{1/2}}. \quad (32) \end{aligned}$$

The detailed derivations are given in the Supplemental Material [74]. We note that these formulas can also be used to calculate long-range interaction coefficients for other two-body or three-body systems such as the two-body Li( $2^2S$ )-Li( $2^2P$ ) system, the two-body Li( $2^2S$ )-Li<sup>+</sup>( $1^1S$ ) system, the two-body Li( $2^2P$ )-Li<sup>+</sup>( $1^1S$ ) system, and the three-body Li( $2^2S$ )-Li( $2^2S$ )-Li<sup>+</sup>( $1^1S$ ) system. We will provide specific examples below in Secs. II G–III.

### F. Second-order nonadditive potentials

Due to the degeneracy of the three-body system, the nonadditive potential  $\Delta E_{\text{non}}^{(2)}$  starts at the second order and is given by

$$\Delta E_{\text{non}}^{(2)} = -\frac{C_{3,3}^{(12,23)}(1, M)}{R_{12}^3 R_{23}^3} - \frac{C_{3,3}^{(23,31)}(1, M)}{R_{23}^3 R_{31}^3} - \frac{C_{3,3}^{(31,12)}(1, M)}{R_{31}^3 R_{12}^3} - \frac{C_{4,2}^{(12,23)}(1, M)}{R_{12}^4 R_{23}^2} - \frac{C_{2,4}^{(31,12)}(1, M)}{R_{31}^2 R_{12}^4} - \dots, \quad (33)$$

where  $C_{3,3}^{(23,31)}(1, M)$  represents the dispersion nonadditive interaction coefficient. The remaining terms are the nonadditive induction interactions. The detailed expressions are given by

$$\begin{aligned} C_{3,3}^{(23,31)}(1, M) = & \sum_{M_u} (-1)^{M_u + M} G_4(1, M_u; 1, M) \{ (a^* b) \exp[i(M_u - M)\gamma] + (b^* a) \exp[-i(M_u - M)\gamma] \} \\ & \times \sum_{n_u} \left[ \frac{|\langle n_0 1 \| T_1 \| n_0 0 \rangle|^2 |\langle n_0 0 \| T_1 \| n_u 1 \rangle|^2}{(E_{n_u 1} - E_{n_0 0}^{(0)}) + (E_{n_0 0} - E_{n_0 1})} + \frac{|\langle n_0 0 \| T_1 \| n_0 1 \rangle|^2 |\langle n_0 0 \| T_1 \| n_u 1 \rangle|^2}{(E_{n_u 1} - E_{n_0 0}^{(0)}) + (E_{n_0 1} - E_{n_0 0})} \right], \quad (34) \end{aligned}$$

$$\begin{aligned} C_{4,2}^{(12,23)}(1, M) = & |a|^2 \sum_{M_t} (-1)^{M_t + M} G_5(1, M_t; 2; 1, M; Q) \cos(M_t \beta) \sum_{n_t} \frac{\langle n_0 1 \| T_2 \| n_0 1 \rangle |\langle n_0 0 \| T_1 \| n_t 1 \rangle|^2}{E_{n_t 1} - E_{n_0 0}} \\ & + \sum_{M_t, m'_2} G_6(2, M_t; 1, m'_2; 1, M; Q) \{ (a^* b) \exp[-i(m'_2)\beta] + (b^* a) \exp[i(m'_2)\beta] \} \end{aligned}$$

$$\begin{aligned}
 & \times \sum_{n_t} \frac{\langle n_0 0 \| T_1 \| n_0 1 \rangle \langle n_0 0 \| T_2 \| n_t 2 \rangle^* \langle n_0 1 \| T_1 \| n_t 2 \rangle}{E_{n_t 2} - E_{n_0 1}} \\
 & - \sum_{M_t} G_7(1, M_t; 2; 1, M; Q) \{ (a^* b) \exp[i(M_t)\beta] + (b^* a) \exp[-i(M_t)\beta] \} \\
 & \times \sum_{n_t} \frac{\langle n_0 0 \| T_1 \| n_0 1 \rangle^* \langle n_0 1 \| T_2 \| n_t 1 \rangle^* \langle n_0 0 \| T_1 \| n_t 1 \rangle}{E_{n_t 1} - E_{n_0 0}}, \tag{35}
 \end{aligned}$$

$$\begin{aligned}
 C_{2,4}^{(31,12)}(1, M) &= |b|^2 \sum_{M_s} (-1)^{M_s+M} G_5(1, M_s; 2; 1, M; Q) \cos(M_s \alpha) \sum_{n_s} \frac{\langle n_0 1 \| T_2 \| n_0 1 \rangle \langle n_0 0 \| T_1 \| n_s 1 \rangle^2}{E_{n_s 1} - E_{n_0 0}} \\
 & + \sum_{M_s m'_1} G_6(2, M_s; 1, m'_1; 1, M; Q) \{ (a^* b) \exp[i(m'_1)\alpha] + (b^* a) \exp[-i(m'_1)\alpha] \} \\
 & \times \sum_{n_s} \frac{\langle n_0 0 \| T_1 \| n_0 1 \rangle \langle n_0 0 \| T_2 \| n_s 2 \rangle^* \langle n_0 1 \| T_1 \| n_s 2 \rangle}{E_{n_s 2} - E_{n_0 1}} \\
 & - \sum_{M_s} G_7(1, M_s; 2; 1, M; Q) \{ (a^* b) \exp[i(M_s)\alpha] + (b^* a) \exp[-i(M_s)\alpha] \} \\
 & \times \sum_{n_s} \frac{\langle n_0 0 \| T_1 \| n_0 1 \rangle^* \langle n_0 1 \| T_2 \| n_s 1 \rangle^* \langle n_0 0 \| T_1 \| n_s 1 \rangle}{E_{n_s 1} - E_{n_0 0}}, \tag{36}
 \end{aligned}$$

$$\begin{aligned}
 C_{3,3}^{(12,23)}(1, M) &= \sum_{M_t m'_2} G_6(1, M_t; 2, m'_2; 1, M; Q) \{ (a^* b) \exp[-i(m'_2)\beta] + (b^* a) \exp[i(m'_2)\beta] \} \\
 & \times \sum_{n_t} \frac{\langle n_0 0 \| T_1 \| n_0 1 \rangle \langle n_0 0 \| T_1 \| n_t 1 \rangle^* \langle n_0 1 \| T_2 \| n_t 1 \rangle}{E_{n_t 1} - E_{n_0 1}} \\
 & - \sum_{M_t} G_7(2, M_t; 1; 1, M; Q) \{ (a^* b) \exp[i(M_t)\beta] + (b^* a) \exp[-i(M_t)\beta] \} \\
 & \times \sum_{n_t} \frac{\langle n_0 0 \| T_1 \| n_0 1 \rangle^* \langle n_0 1 \| T_1 \| n_t 2 \rangle^* \langle n_0 0 \| T_2 \| n_t 2 \rangle}{E_{n_t 2} - E_{n_0 0}}, \tag{37}
 \end{aligned}$$

and

$$\begin{aligned}
 C_{3,3}^{(31,12)}(1, M) &= \sum_{M_s m'_1} G_6(1, M_s; 2, m'_1; 1, M; Q) \{ (a^* b) \exp[i(m'_1)\alpha] + (b^* a) \exp[-i(m'_1)\alpha] \} \\
 & \times \sum_{n_s} \frac{\langle n_0 0 \| T_1 \| n_0 1 \rangle \langle n_0 0 \| T_1 \| n_s 1 \rangle^* \langle n_0 1 \| T_2 \| n_s 1 \rangle}{E_{n_s 1} - E_{n_0 1}} \\
 & - \sum_{M_s} G_7(2, M_s; 1; 1, M; Q) \{ a^* b \exp[i(M_s)\alpha] + b^* a \exp[-i(M_s)\alpha] \} \\
 & \times \sum_{n_s} \frac{\langle n_0 0 \| T_1 \| n_0 1 \rangle^* \langle n_0 1 \| T_1 \| n_s 2 \rangle^* \langle n_0 0 \| T_2 \| n_s 2 \rangle}{E_{n_s 2} - E_{n_0 0}}, \tag{38}
 \end{aligned}$$

where the functions  $G_4, G_5, G_6,$  and  $G_7$  are defined by

$$G_4(L_i, M_i; L, M) = 16\pi^2 \frac{[P_{L_i+L}^{M_i-M}(0)(L_i+L-M_i+M)!(L_i, L)^{-1}]^2}{(L_i+M_i)!(L_i-M_i)!(L+M)!(L-M)!}, \tag{39}$$

$$G_5(L_i, M_i; \ell_k, L, M; Q) = \frac{8\sqrt{\pi^3} Q P_{\ell_k+L_i}^{M_i}(0) P_{L_i}^{M_i}(0) (\ell_k+L_i-M_i)!}{(2L_i+1)^2 \sqrt{2\ell_k+1} (l_1)! (L_i+M_i)!} \begin{pmatrix} L & \ell_k & L \\ -M & 0 & M \end{pmatrix}, \tag{40}$$

$$\begin{aligned}
 G_6(L_i, M_i; \ell_k, m_k; L, M; Q) &= \frac{8\sqrt{\pi^3} Q (\ell_k)^{-1/2}}{(2L+1)(2L_i+1)} \begin{pmatrix} L & \ell_k & L_i \\ -M & -m_k & M_i \end{pmatrix} \\
 & \times \frac{P_{L+L_i}^{-M+M_i}(0) P_{\ell_k}^{m_k}(0) (L+L_i+M-M_i)! (\ell_k-m_k)!}{[(L+M)!(L-M)!(L_i+M_i)!(L_i-M_i)!(\ell_k+m_k)!(\ell_k-m_k)!]^{1/2}}, \tag{41}
 \end{aligned}$$

$$G_7(L_i, M_i; \ell_k; L, M; Q) = \frac{8\sqrt{\pi^3}Q(\ell_k)^{-1/2}}{(2L+1)(2L_i+1)} \sum_{m_k} \begin{pmatrix} L & \ell_k & L_i \\ -M & m_k & M_i \end{pmatrix} \times \frac{P_{L+\ell_k}^{M-m_k}(0)P_{L_i}^{M_i}(0)(L+\ell_k-M+m_k)!(L_i-M_i)!}{[(L+M)!(L-M)!(L_i+M_i)!(L_i-M_i)!(\ell_k+m_k)!(\ell_k-m_k)!]^{1/2}}. \quad (42)$$

The detailed derivations are given in the Supplemental Material [74]. From Eqs. (18)–(38) we see that all of these coefficients depend on the atomic states of the three-body system because they include  $a$  and  $b$ . In other words, these additive and nonadditive coefficients show a dependence on the configurations of the three-body system. This is clearly a kind of quantum three-body collective effect. In the following section we show that these three-body nonadditive interactions significantly influence the total interaction potentials. Because of the enhancement through the induction effect, the nonadditive interactions are large enough to be comparable to (or even stronger than) the additive interactions at the same order.

In the present paper we only consider long-range interaction for the  $\text{Li}(2^2S)\text{-Li}(2^2P)\text{-Li}^+(1^1S)$  system up to  $O(R^{-6})$ , since the next terms are  $C_7/R^7$ , which come from the third-order perturbation theory.

### G. Specific results extracted from the general expressions

With the zeroth-order wave functions as shown in Eq. (15), the present work can be easily related to the calculations of long-range interactions for other two-body or three-body systems. For example, if we set  $a = 1$  and  $b = 0$  and remove the terms involving the  $\text{Li}^+(1^1S)$  ion, the formulas can be used to describe the long-range interactions for the two-body  $\text{Li}(2^2S)\text{-Li}(2^2S)$  system; if we set  $a = \frac{1}{\sqrt{2}}$  and  $b = \pm \frac{1}{\sqrt{2}}$  and remove the terms involving the  $\text{Li}^+(1^1S)$  ion, the formulas can be used to describe the long-range interactions for the two-body  $\text{Li}(2^2S)\text{-Li}(2^2P)$  system; if we set  $a = 1$  and  $b = 0$  and remove the terms involving the  $\text{Li}(2^2P)$  atom, the formulas can be used to describe the long-range interactions for the two-body  $\text{Li}(2^2S)\text{-Li}^+(1^1S)$  system; if we set  $a = 1$  and  $b = 0$  and remove the terms involving the  $\text{Li}(2^2S)$  atom, the formulas can be used to describe the long-range interactions for the two-body  $\text{Li}(2^2P)\text{-Li}^+(1^1S)$  system; and if we set  $a = 1$ ,  $b = 0$ , and  $L = 0$ , the formulas can be used to describe the long-range interactions for the three-body  $\text{Li}(2^2S)\text{-Li}(2^2S)\text{-Li}^+(1^1S)$  system. For these long-range *additive* interaction coefficients, we have arranged the formulas to show these connections,

$$C_3^{(12)}(1, M) = C_{3,\text{dip}}^{(P-S)}, \quad (43)$$

$$C_3^{(23)}(1, M) = |b|^2 C_{3,\text{elst}}^{(P-S^+)}, \quad (44)$$

$$C_3^{(31)}(1, M) = |a|^2 C_{3,\text{elst}}^{(P-S^+)}, \quad (45)$$

$$C_4^{(23)}(1, M) = |a|^2 C_{4,\text{ind}}^{(S-S^+)} + |b|^2 C_{4,\text{ind}}^{(P-S^+)}, \quad (46)$$

$$C_4^{(31)}(1, M) = |a|^2 C_{4,\text{ind}}^{(P-S^+)} + |b|^2 C_{4,\text{ind}}^{(S-S^+)}, \quad (47)$$

$$C_6^{(12)}(1, M) = C_{6,\text{disp}}^{(P-S)}, \quad (48)$$

$$C_6^{(23)}(1, M) = |a|^2 \{C_{6,\text{ind}}^{(S-S^+)} + C_{6,\text{disp}}^{(S-S^+)}\} + |b|^2 \{C_{6,\text{ind}}^{(P-S^+)}(M) + C_{6,\text{disp}}^{(P-S^+)}(M)\}, \quad (49)$$

and

$$C_6^{(31)}(1, M) = |a|^2 \{C_{6,\text{ind}}^{(P-S^+)}(M) + C_{6,\text{disp}}^{(P-S^+)}(M)\} + |b|^2 \{C_{6,\text{ind}}^{(S-S^+)} + C_{6,\text{disp}}^{(S-S^+)}\}, \quad (50)$$

where  $C_{3,\text{dip}}^{(P-S)}$  and  $C_{6,\text{disp}}^{(P-S)}$  represent the dipolar and dispersion interaction coefficients for the two-body  $\text{Li}(2^2S)\text{-Li}(2^2P)$  system, respectively, which have been given in the Ref. [10] [also see Eqs. (51) and (52) in the Supplemental Material [74]]. In addition,  $C_{2n,\text{ind}}^{(S-S^+)}$  and  $C_{2n,\text{disp}}^{(S-S^+)}$  represent the long-range induction and dispersion coefficients for the  $\text{Li}(2^2S)\text{-Li}^+(1^1S)$  system, which have been given in the Ref. [12] [also see Eqs. (48)–(50) in the Supplemental Material [74]]. For the two-body  $\text{Li}(2^2P)\text{-Li}^+(1^1S)$  system, we provide more details below in Sec. III. In short,  $C_{3,\text{elst}}^{(P-S^+)}$  represents the electrostatic interaction between the charge of the ion and the quadrupole moment of the neutral atom;  $C_{2n,\text{ind}}^{(P-S^+)}$  and  $C_{2n,\text{disp}}^{(P-S^+)}$  represent the long-range induction and dispersion coefficients for the  $\text{Li}(2^2P)\text{-Li}^+(1^1S)$  system, where the formulas of these coefficients are given by Eqs. (56)–(60) in Sec. III. Clearly, with these formulas, we can easily relate the long-range additive interactions of the three-body  $\text{Li}(2^2S)\text{-Li}(2^2P)\text{-Li}^+(1^1S)$  system to those of other two-body or three-body systems. On the other hand, the *nonadditive* interactions of the three-body  $\text{Li}(2^2S)\text{-Li}(2^2P)\text{-Li}^+(1^1S)$  system are induced by the degeneracy and cannot be decomposed in terms of diatomic subsystems. This is in contrast to the nondegenerate  $\text{Li}(2^2S)\text{-Li}(2^2S)\text{-Li}^+(1^1S)$  system [12], where the nonadditive interactions start from the third-order energy correction and may still be used to predict contributions to the long-range potentials between the  $\text{Li}(2^2S)$  atom and the excited-state dimer  $\text{Li}_2^+(2^2\Sigma_{g,u}^+, 1^2\Sigma_{g,u})$  or between the  $\text{Li}(2^2P)$  atom and the ground-state dimer  $\text{Li}_2^+(1^2\Sigma_{g,u}^+)$ . We note that  $C_{4,2}^{(12,23)}(1, M)$  [see Eq. (35)] and  $C_{2,4}^{(31,12)}(1, M)$  [see Eq. (36)] may be very important in the study of the interactions between the cation  $\text{Li}^+(1^1S)$  and the excited dimer  $\text{Li}_2^+(2^2\Sigma_{g,u}^+, 1^2\Sigma_{g,u})$ .

### H. Orientation dependence

In this section we describe the orientation dependence of the long-range interactions due to the anisotropic charge distribution of the excited Li atom. To illustrate the orientation

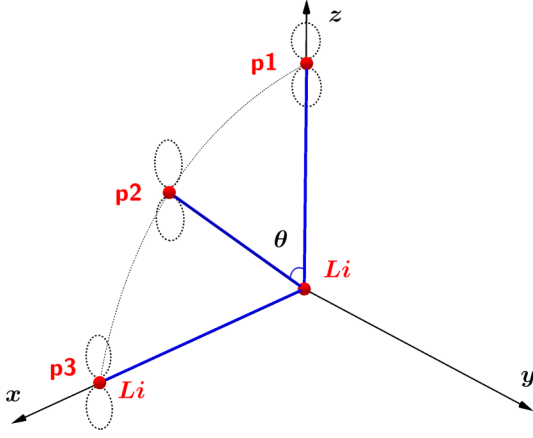


FIG. 2. Simple illustration of the rotation of the two-body system from the  $z$  axis to the  $x$  axis. Here  $p_1$ ,  $p_2$ , and  $p_3$  represent positions 1, 2, and 3, respectively.

dependence, we use the two-body  $\text{Li}(2^2S)\text{-Li}(2^2P)$  system as an example. The rotation of the two-body system is illustrated in Fig. 2, where the two-body system is rotated from the  $z$  axis to the  $x$  axis (or one of the two atoms is rotated from  $p_1$  to  $p_3$ ). In this process, we find that the zeroth-order wave functions of the two-body system  $\Psi_{S-P}^{(0)}(M)$  and the corresponding long-range interaction coefficients change. Thus we can easily get the inequality relation

$$C_{n,p_1}^{(S-P)}(M) \neq C_{n,p_2}^{(S-P)}(M) \neq C_{n,p_3}^{(S-P)}(M). \quad (51)$$

In our previous work we have given the numerical values of the long-range interaction coefficients for the two atoms lying on the  $z$  axis (see Table IX in Ref. [70]), which would correspond to  $p_3$  in Fig. 2. In the present work we use the coordinates of Fig. 1, represented as  $p_1$  in Fig. 2, which corresponds to the two atoms lying on the  $x$  axis. The comparison of these long-range interaction coefficients is given in Table I, where the present values were obtained using highly accurate variational wave functions for the Li atom in Hylleraas coordinates with finite nuclear mass effects [70]. For these two specific situations ( $p_1$  and  $p_3$ ), we also find the relations

$$C_{n,p_3}^{(S-P)}(M=0) = C_{n,p_1}^{(S-P)}(M=\pm 1), \quad (52)$$

which are obeyed by our numerical values of these coefficients shown in Table I.

TABLE I. Long-range interaction coefficients (in a.u.) of the  ${}^\infty\text{Li}(2^2S)\text{-}{}^\infty\text{Li}(2^2P)$  system for the two atoms lying on the  $z$  axis and the  $x$  axis, respectively. Here  $p_1$  and  $p_3$  are as shown in Fig. 2. The numbers in parentheses represent the computational uncertainties.

	$C_{3,z}^{(S-P)}(M=0)$	$C_{3,z}^{(S-P)}(M=\pm 1)$	$C_{6,z}^{(S-P)}(M=0)$	$C_{6,z}^{(S-P)}(M=\pm 1)$
$p_1$				
$\Psi_{S-P,z}^{(0)}(\beta=1)$	11.000221(2)	-5.500111(1)	2075.40(3)	1406.68(3)
$\Psi_{S-P,z}^{(0)}(\beta=-1)$	-11.000221(2)	5.500111(1)	2075.40(3)	1406.68(3)
$p_3$				
	$C_{3,x}^{(S-P)}(M=0)$	$C_{3,x}^{(S-P)}(M=\pm 1)$	$C_{6,x}^{(S-P)}(M=0)$	$C_{6,x}^{(S-P)}(M=\pm 1)$
$\Psi_{S-P,x}^{(0)}(\beta=1)$	-5.500111(1)	2.750054(1)	1406.68(3)	1741.06(5)
$\Psi_{S-P,x}^{(0)}(\beta=-1)$	5.500111(1)	-2.750054(1)	1406.68(3)	1741.06(5)

In general, the long-range interaction coefficients are given by

$$C_{n,p_i}^{(S-P)}(M) = C_{n,p_i}^{(S-P)}(M, \cos \theta_i), \quad (53)$$

where  $p_i$  is the position  $i$  of the atom as shown in Fig. 2 and  $\theta_i$  is the corresponding polar angle. For the leading coefficients  $C_3$ , the formulas are simplified as

$$C_{3,p_i}^{(S-P)}(M) = C_{3,p_i}^{(S-P)}(M)P_2(\cos \theta_i), \quad (54)$$

where  $P_2(\cos \theta_i)$  is the Legendre polynomial. For the other coefficients  $C_n$  with  $n > 3$ , the parts containing the polar angle  $\theta_i$  would be coupled with the virtual states, which cannot be separated. However, we can still utilize the present formulas (calculated at the  $p_1$  orientation) to give the general formulas by changing the Legendre polynomial from  $P_l^m(0)$  to  $P_l^m(\cos \theta_i)$ . For example, we can use the formula of Eq. (52) in the Supplemental Material [74] to get the general leading dispersion coefficient  $C_{6,p_i}^{(S-P)}(M)$  at orientation  $p_i$ . Similarly, for other excited Li dimer and trimers, the long-range interactions also contain such orientation dependences. In the next section we will apply these ideas to derive the long-range potentials for the  $\text{Li}(2^2P)\text{-Li}^+(1^1S)$  system in the  $p_3$  orientation. In Sec. III we will consider the three-body system in detail.

### I. Long-range potentials for the $\text{Li}(2^2P)\text{-Li}^+(1^1S)$ system

In this section we use our results to calculate the long-range potentials of the four states of  $\text{Li}_2^+$ ,  $1^2\Pi_u$ ,  $1^2\Pi_g$ ,  $2^2\Sigma_g^+$ , and  $2^2\Sigma_u^+$ , correlating to the  $\text{Li}(2^2P)\text{-Li}^+(1^1S)$  system. We begin by writing down the long-range potential as calculated in our coordinates (see Fig. 1), with  $V^{(P-S^+)}(R; M)$  corresponding to the two-body  $\text{Li}(2^2P)\text{-Li}^+(1^1S)$  system in the orientation  $p_3$  of Fig. 2, which can be written as

$$V^{(P-S^+)}(R; M) = -\frac{C_3(M)}{R^3} - \frac{C_4(M)}{R^4} - \frac{C_6(M)}{R^6} - \dots, \quad (55)$$

where  $C_3(M)$  represents the electrostatic interaction between the charge of the  $\text{Li}^+(1^1S)$  ion and the quadrupole moment of the excited  $\text{Li}(2^2P)$  atom,  $C_4(M)$  represents the leading long-range induction coefficient, which is related to the dipole polarizability of the  $\text{Li}(2^2P)$  atom, and  $C_6(M)$  is the sum of long-range induction coefficients  $C_{6,\text{ind}}$  and dispersion coefficients  $C_{6,\text{disp}}$ . The formulas of these coefficients are

given by

$$C_3(M) = C_{3,\text{elst}}^{(P-S^+)}(M) = Q(-1)^{1+M} \sqrt{\frac{\pi}{5}} \begin{pmatrix} 1 & 2 & 1 \\ -M & 0 & M \end{pmatrix} \langle n_0 1 \| T_2 \| n_0 1 \rangle, \quad (56)$$

$$C_4(M) = C_{4,\text{ind}}^{(P-S^+)}(M) = \frac{Q^2}{4\pi} \sum_{n_i L_i} \frac{G_1(L_i, 0; 1, 1; 1, M) |\langle n_0 1 \| T_1 \| n_i L_i \rangle|^2}{E_{n_i L_i} - E_{n_0 1}^{(0)}}, \quad (57)$$

$$C_6(M) = C_{6,\text{disp}}^{(P-S^+)}(M) + C_{6,\text{ind}}^{(P-S^+)}(M), \quad (58)$$

where

$$C_{6,\text{disp}}^{(P-S^+)}(M) = \sum_{n_i n_u L_i} \frac{G_1(L_i, 1; 1, 1; 1, M) |\langle n_0 1 \| T_1 \| n_i L_i \rangle|^2 \langle n'_0 0 \| T_1 \| n_u 1 \rangle^2}{(E_{n_i L_i} - E_{n_0 1}^{(0)}) + (E_{n_u 1} - E_{n'_0 0}^{(0)})} \quad (59)$$

and

$$C_{6,\text{ind}}^{(P-S^+)}(M) = \frac{Q^2}{4\pi} \sum_{n_i n_u L_i} \left\{ \frac{G_1(L_i, 0; 2, 2; 1, M) |\langle n_0 1 \| T_2 \| n_i L_i \rangle|^2}{E_{n_i L_i} - E_{n_0 1}^{(0)}} + \frac{G_1(L_i, 0; 1, 3; 1, M) \langle n_0 1 \| T_1 \| n_i L_i \rangle^* \langle n_0 1 \| T_3 \| n_i L_i \rangle}{E_{n_i L_i} - E_{n_0 1}^{(0)}} \right. \\ \left. + \frac{G_1(L_i, 0; 3, 1; 1, M) \langle n_0 1 \| T_3 \| n_i L_i \rangle^* \langle n_0 1 \| T_1 \| n_i L_i \rangle}{E_{n_i L_i} - E_{n_0 1}^{(0)}} \right\} \quad (60)$$

and the  $G_1$  function is defined in Eq. (32).

The molecular states for  $\text{Li}_2^+$  correlating to the  $\text{Li}(2^2P)\text{-Li}^+(1^1S)$  system are the  $2^2\Sigma_g^+$ ,  $2^2\Sigma_u^+$ ,  $1^2\Pi_g$ , and  $1^2\Pi_u$  states (we do not consider fine structure). We calculated the long-range interaction coefficients using Eqs. (56)–(60), which include electrostatic, induction, and dispersion energies up to  $O(R^{-6})$ . These correspond to position p3 of the  $\text{Li}(2^2P)$  atom as indicated in Fig. 2. Convergence studies of these long-range interaction coefficients  $C_{3,x}^{(P-S^+)}(M)$ ,  $C_{4,x}^{(P-S^+)}(M)$ , and  $C_{6,x}^{(P-S^+)}(M)$  are given in Tables II, III, and IV, respectively. In these tables,  $N_P$  denotes the size of the basis for the  $P$  state of the  $^\infty\text{Li}$  atom and  $N_L$  denotes the size of the basis for the corresponding intermediate states of symmetry  $L$ . Similarly,  $N_S^+$  and  $N_P^+$  denote the sizes of the bases for the ground state and the intermediate states of symmetry  $P$  of the  $^\infty\text{Li}^+$  ion, respectively.

In order to apply the results to the  $\Sigma$  and  $\Pi$  molecular states of standard molecular nomenclature, where the  $z$  axis joins the atom and ion, we must first apply the considerations of Sec. IIH to express our results in terms of position p1 of Fig. 2. The analysis yields the coefficients, with the numerical values given in Table V and the corresponding long-range po-

TABLE II. Convergence of the long-range interaction coefficients  $C_{3,x}^{(P-S^+)}(M)$  for the  $^\infty\text{Li}(2^2P)\text{-}^\infty\text{Li}^+(1^1S)$  system, where two particles lie on the  $x$  axis (p3) as shown in Fig. 2. Here  $N_P$  denotes the size of the basis for the  $P$  state of the  $^\infty\text{Li}(2^2P)$  atom.

$N_P$	$C_{3,x}^{(P-S^+)}(M=0)$	$C_{3,x}^{(P-S^+)}(M=\pm 1)$
1174	−5.409965844	2.704982922
2091	−5.409968720	2.704984360
3543	−5.409969427	2.704984713
5761	−5.409969563	2.704984781
extrapolated	−5.4099696(1)	2.7049847(1)

tentials given in Fig. 3. The corresponding general coefficients are defined by

$$C_{3,p_i}^{(P-S^+)}(M) = C_{3,p_i}^{(P-S^+)}(M) P_2(\cos \theta_i), \quad (61)$$

$$C_{4,p_i}^{(P-S^+)}(M=0) = \frac{1}{2} \alpha_{zz}^{p_i} = \frac{1}{2} [\alpha_1 - 2\alpha_{1,p_1}^T P_2(\cos \theta_i)], \quad (62)$$

and

$$C_{4,p_i}^{(P-S^+)}(M=\pm 1) = \frac{1}{2} \alpha_{xx}^{p_i} = \frac{1}{2} [\alpha_1 + \alpha_{1,p_1}^T P_2(\cos \theta_i)], \quad (63)$$

where  $\alpha_{zz}^{p_i}$  and  $\alpha_{xx}^{p_i}$  are the polarizability components along the  $z$  and  $x$  directions of an applied electric field [75–78], respectively,  $\alpha_1$  and  $\alpha_1^T$  are the principal scalar and tensor polarizabilities of the  $\text{Li}(2^2P)$  atom [70], and  $P_2(\cos \theta_i)$  is the Legendre polynomial. The comparison of the polarizability components  $\alpha_{zz}^{p_1}$  and  $\alpha_{xx}^{p_1}$ , and  $\alpha_{zz}^{p_3}$  and  $\alpha_{xx}^{p_3}$  is given in Table VI. In the present configuration (as shown in Fig. 1), these components can be related to the leading induction coefficients  $C_{4,x}(M)$  (as shown in Table V) by  $\alpha_{zz}^{p_3} = 2C_{4,x}(M=0)$  and  $\alpha_{xx}^{p_3} = 2C_{4,x}(M=\pm 1)$ . According to the symmetry of the degenerate system [75–78], we can connect the polarizability

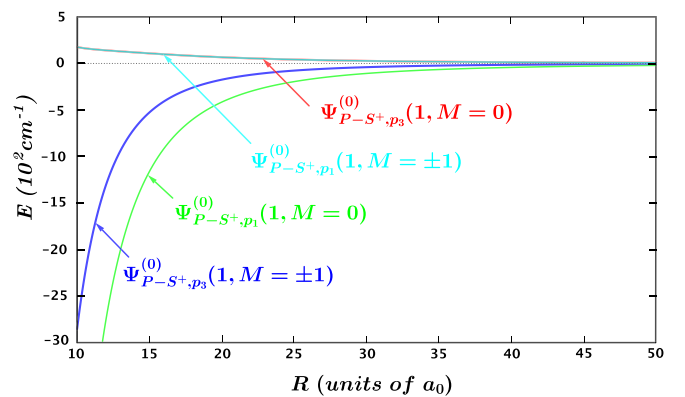


FIG. 3. Long-range potentials (in a.u.) of the  $\text{Li}(2^2P)\text{-Li}^+(2^1S)$  system calculated in the coordinate system of Fig. 1, which corresponds to p3 of Fig. 2.

TABLE III. Convergence of the long-range interaction coefficients  $C_{4,x}^{(P-S^+)}(M)$  for the  ${}^\infty\text{Li}(2^2P)\text{-}{}^\infty\text{Li}^+(1^2S)$  system, where two particles lie on the  $x$  axis (p3) as shown in Fig. 2. Here  $N_P$  denotes the size of basis for the  $P$  state of the  ${}^\infty\text{Li}$  atom. In addition,  $N_S$ ,  $N_{(pp)P}$ , and  $N_D$  denote the sizes of the bases for the corresponding intermediate states of symmetries  $S$ ,  $P$ , and  $D$ , respectively, and  $(pp)P$  stands for the main configuration of two  $p$  electrons coupled to form a total angular momentum of  $P$  [since the contribution from the  $(pp)P$  configuration converges at  $N_{(pp)P} = 3413$ , we did not increase  $N_{(pp)P}$  any further [70]].

$(N_P, N_S, N_{(pp)P}, N_D)$	$C_{4,x}^{(P-S^+)}(M = 0)$	$C_{4,x}^{(P-S^+)}(M = \pm 1)$
(1174,1589,1106,1174)	64.282596	63.061604
(2091,2625,2002,2091)	64.283174	63.066184
(3543,4172,3413,3543)	64.283498	63.067033
(5761,6412,3413,5761)	64.283634	63.067338
extrapolated	64.2838(2)	63.0676(3)

components  $\alpha_{zz}^{P_3}$  and  $\alpha_{xx}^{P_3}$  with the principal polarizabilities, scalar ( $\alpha_1$ ) and tensor ( $\alpha_2^T$ ), of the  $\text{Li}(2^2P)$  atom by  $\alpha_1 = \frac{1}{3}(\alpha_{zz}^{P_3} + 2\alpha_{xx}^{P_3})$  and  $\alpha_2^T = \frac{2}{3}(\alpha_{zz}^{P_3} - \alpha_{xx}^{P_3})$ . For example, using the present data from Table VI, we find  $\alpha_1 = 126.9460$  and  $\alpha_2^T = 1.6216$  in agreement with Table VIII in Ref. [70]. Further details concerning the polarizability components  $\alpha_{zz}^{P_1}$  and  $\alpha_{xx}^{P_1}$  for the two particles lying on the  $z$  axis are given in, for example, Refs. [75–78]. For the coefficient  $C_6$ , we can use the formula of Eq. (58) by changing the Legendre polynomial from  $P_l^m(0)$  to  $P_l^m(\cos\theta_i)$  to get the general  $C_{6,p_i}^{(P-S^+)}(M)$  at orientation  $p_i$ .

The long-range potential energy functions expressed relative to p1 follow from Table V. For example, for the  $2^2\Sigma_{g,u}$  states of the  ${}^\infty\text{Li}_2$  we have

$$V^{(P-S^+)}(R; \Sigma) = -\frac{10.8199392}{R^3} - \frac{61.8515}{R^4} - \frac{9811.485}{R^6} - \dots, \quad (64)$$

and for the  $1^1\Pi_{g,u}$  states we have

$$V^{(P-S^+)}(R; \Pi) = \frac{5.4099696}{R^3} - \frac{64.2838}{R^4} + \frac{1820.6261}{R^6} - \dots. \quad (65)$$

Similar expressions may be written for  ${}^6\text{Li}_2^+$  and  ${}^7\text{Li}_2^+$  using Table V.

Magnier *et al.* [54] calculated the long-range potentials with the inclusion of exchange, electrostatic, induction, and dispersion interactions up to  $O(R^{-8})$ ; the results were presented graphically. While a direct comparison of long-range

coefficients is not possible, we can calculate the exchange energies using the expressions given by Magnier *et al.* and add those to our long-range potentials to compare with their total potentials for each of the four molecular states. When the exchange energy and the long-range potential energy have opposite signs, a long-range well or barrier results; these singular features provide good quantitative checks between the calculations of Magnier *et al.* and the present work. From Figs. 8–10 in [54] it is evident that the exchange energies are positive for the  $2^2\Sigma_u^+$  and  $1^2\Pi_g$  states and negative for the  $2^2\Sigma_g^+$  and  $1^2\Pi_u$  states, while the exchange splitting for the pair of  $2^2\Sigma^+$  states is larger by a factor of  $R/2$  compared to the pair of  $1^2\Pi$  states, where  $R$  is the internuclear distance. Calculations show that the two  $\Sigma$  states and the  $1^2\Pi_u$  state form potential wells, while the  $1^2\Pi_g$  state is purely repulsive [55]. It is evident from the data in Eq. (65) that the net positive long-range potential and positive exchange energy completely account for the repulsive  $1^2\Pi_g$  state. Of the three states with potential wells, the  $2^2\Sigma_u^+$  state well exists at the greatest internuclear distance, about  $25a_0$ , with a depth of only  $127\text{ cm}^{-1}$  according to a recent model potential calculation [55]. With our long-range expansion of Table V evaluated for  ${}^\infty\text{Li}$  as in Eq. (64) and using Eq. (8) of Ref. [54], to estimate the contribution of the exchange energy<sup>2</sup> we find a

<sup>2</sup>By a close comparison of Eqs. (2.13) and (3.7) of Ref. [82], we believe that the factor 2 in the denominator of  $D$  given in Eq. (8) of Ref. [54] should be replaced by  $m!$ . We evaluated the exchange energy splittings with this evident correction included.

TABLE IV. Convergence of the long-range interaction coefficients  $C_{6,x}^{(P-S^+)}(M)$  for the  ${}^\infty\text{Li}(2^2P)\text{-}{}^\infty\text{Li}^+(1^2S)$  system, where two particles lie on the  $x$  axis (p3) as shown in Fig. 2. Here  $N_P$  denotes the sizes of bases for the  $P$  state of the  ${}^\infty\text{Li}$  atom. In addition,  $N_S$ ,  $N_{(pp)P}$ , and  $N_D$  are the sizes of basis for the corresponding intermediate states of symmetries  $S$ ,  $P$ , and  $D$ , respectively, and  $(pp)P$  stands for the main configuration of two  $p$  electrons coupled to form a total angular momentum of  $P$  [since the contribution from the  $(pp)P$  configuration converges at  $N_{(pp)P} = 3413$ , we did not increase  $N_{(pp)P}$  any further [70]]. Further,  $N_S^+$  and  $N_P^+$  denote the sizes of the bases for the ground state and the intermediate states, respectively, of symmetry  $P$  of  ${}^\infty\text{Li}^+$ .

$(N_S^+, N_P^+; N_P, N_S, N_{(pp)P}, N_D)$	$C_{6,x}^{(P-S^+)}(M = 0)$	$C_{6,x}^{(P-S^+)}(M = \pm 1)$
(504,728,1174,1589,1106,1174)	−1820.631774	3995.37910
(744,1120,2091,2625,2002,2091)	−1820.627179	3995.40911
(1050,1632,3543,4172,3413,3543)	−1820.626701	3995.42357
(1430,2280,5761,6412,3413,5761)	−1820.626499	3995.42669
extrapolated	−1820.6261(3)	3995.429(3)

TABLE V. Long-range interaction coefficients (in a.u.) of the Li( $2^2P$ )-Li $^+$ ( $1^2S$ ) system for the two particles lying on the  $z$  axis and the  $x$  axis, respectively. Here p1 and p3 are as shown in Fig. 2. Position p1 corresponds to standard molecular  $\Sigma$  and  $\Pi$  nomenclature where the  $z$  axis joins the atom and the ion. The numbers in parentheses represent the computational uncertainties.

p1	$C_{3,z}^{(P-S^+)}(M=0)$	$C_{3,z}^{(P-S^+)}(M=\pm 1)$	$C_{4,z}^{(P-S^+)}(M=0)$	$C_{4,z}^{(P-S^+)}(M=\pm 1)$	$C_{6,z}^{(P-S^+)}(M=0)$	$C_{6,z}^{(P-S^+)}(M=\pm 1)$
$^\infty\text{Li}$	10.8199392(2)	-5.4099696(1)	61.8515(2)	64.2838(2)	9811.485(6)	-1820.6261(3)
$^7\text{Li}$	10.8192592(2)	-5.4096296(1)	61.8385(2)	64.2911(2)	9811.274(6)	-1820.7205(2)
$^6\text{Li}$	10.8191462(2)	-5.4095731(1)	61.8364(2)	64.2925(2)	9811.239(6)	-1820.7362(3)
p3	$C_{3,x}^{(P-S^+)}(M=0)$	$C_{3,x}^{(P-S^+)}(M=\pm 1)$	$C_{4,x}^{(P-S^+)}(M=0)$	$C_{4,x}^{(P-S^+)}(M=\pm 1)$	$C_{6,x}^{(P-S^+)}(M=0)$	$C_{6,x}^{(P-S^+)}(M=\pm 1)$
$^\infty\text{Li}$	-5.4099696(1)	2.7049847(1)	64.2838(2)	63.0676(3)	-1820.6261(3)	3995.429(3)
$^7\text{Li}$	-5.4096296(1)	2.7048148(1)	64.2911(2)	63.0648(2)	-1820.7205(2)	3995.276(3)
$^6\text{Li}$	-5.4095731(1)	2.7047866(1)	64.2925(2)	63.0643(3)	-1820.7362(3)	3995.251(3)

well of depth  $119\text{ cm}^{-1}$  at  $R = 25.8a_0$  to be compared to the depth  $124\text{ cm}^{-1}$  at  $25.7a_0$  obtained by Magnier *et al.* using a long-range expansion and the exchange energy. We also obtain for the  $1^2\Pi_u$  state using Eq. (65) a potential barrier of  $36\text{ cm}^{-1}$  at  $R = 23.9a_0$ , compared to  $40\text{ cm}^{-1}$  at  $23.4a_0$  found by Magnier *et al.* The agreement of the well and the barrier positions and energies calculated using Eqs. (64) and (65) with the similar calculations of Magnier *et al.* is satisfactory. The  $2^2\Sigma_u^+$  state is an example of a long-range molecular state [83]. Moreover, we do not attempt to reproduce the wells of the  $2^2\Sigma_u^+$  or  $1^2\Pi_u$  states, because it is evident from Figs. 8 and 9 in Ref. [54] that these potential wells are fully realized with the inclusion of charge overlap (i.e., in quantum-chemical calculations [54,55]).

Having thus demonstrated that two-body long-range interaction potentials can be extracted from our results, as well as providing the coefficients from Table V and Eqs. (64) and (65), we return to the three-body system.

TABLE VI. Comparison of the polarizability components  $\alpha_{zz}^{p1}$  and  $\alpha_{xx}^{p1}$ , and  $\alpha_{zz}^{p3}$  and  $\alpha_{xx}^{p3}$  (in a.u.) for the excited state  $2^2P$  of  $^\infty\text{Li}$ . For the two coordinate systems, we have  $\alpha_{xx}^{p1} = \alpha_1 + \alpha_1^T$  or  $\alpha_{zz}^{p1} = \alpha_1 - 2\alpha_1^T$  (see Refs. [75–78]) and  $\alpha_{zz}^{p3} = \alpha_1 + \alpha_1^T$  or  $\alpha_{xx}^{p3} = \alpha_1 - \frac{1}{2}\alpha_1^T$ , respectively, where the electric field lies in the  $z$  or  $x$  direction, expressed in terms of the principal polarizabilities  $\alpha_1$  (scalar) and  $\alpha_1^T$  (tensor).

Reference	$\alpha_{zz}^{p1} = 2C_{4,z}^{(P-S^+)}(M=0)$	$\alpha_{xx}^{p1} = 2C_{4,z}^{(P-S^+)}(M=\pm 1)$
Pipin and Bishop [79]	123.634	128.449
Rérat <i>et al.</i> [77]	131	129
Cohen and Themelis [80]	122.94	128.13
Johnson <i>et al.</i> [81]	123.81	128.580
this work	123.703(4)	128.5676(4)
Reference	$\alpha_{zz}^{p3} = 2C_{4,x}^{(P-S^+)}(M=0)$	$\alpha_{xx}^{p3} = 2C_{4,x}^{(P-S^+)}(M=\pm 1)$
Pipin and Bishop [79]	128.449	126.0415
Rérat <i>et al.</i> [77]	129	131
Cohen and Themelis [80]	128.13	125.535
Johnson <i>et al.</i> [81]	128.580	126.195
this work	128.5676(4)	126.1352(6)

### III. RESULTS AND DISCUSSION

As in Secs. IIH and III, we use highly accurate variational wave functions for lithium atoms and ions in Hylleraas coordinates with finite nuclear mass effects to evaluate the numerical values [70]. We note that in general the zeroth-order wave functions are obtained by using degenerate perturbation theory through Eq. (10) in the Supplemental Material [74] and there are intrinsic geometrical dependences that complicate the analysis. In particular, the zeroth-order wave functions change with the geometry (interior angles and interatomic separations) of the three-body system. However, when  $R_{23} = R_{31} = R$ , we have the matrix elements  $\Delta_{12} = \Delta_{21}$  [see Eq. (10) in the Supplemental Material [74]] and the geometrical dependences do not appear in the zeroth-order wave functions, simplifying the analysis of the three-body system. Therefore, in this section we consider the Li( $2^2S$ )-Li( $2^2P$ )-Li $^+$ ( $1^1S$ ) system for the configurations where  $R_{23} = R_{31} = R$ .

In Sec. III A we introduce the zeroth-order wave functions and in Sec. III B provide the numerical values of these additive coefficients. In Sec. III C we focus on the two specific arrangements of the three particles, collinear and in an equilateral triangle, providing the nonadditive coefficients.

#### A. Additive coefficients: Wave functions

With respect to the p1 orientation as shown in Fig. 2, we calculate the long-range additive potentials for the three-body system lying collinearly on the  $z$  axis. According to degenerate perturbation theory, the corresponding zeroth-order wave functions are

$$\Psi_{1,z}^{(0)} = \frac{1}{\sqrt{2}}[|n_0 1_z; n_0 0; n'_0 0\rangle + |n_0 0; n_0 1_z; n'_0 0\rangle], \quad (66)$$

$$\Psi_{2,z}^{(0)} = \frac{1}{\sqrt{2}}[|n_0 1_z; n_0 0; n'_0 0\rangle - |n_0 0; n_0 1_z; n'_0 0\rangle], \quad (67)$$

where the symbol  $z$  indicates the three-particles lying on the  $z$  axis for the configurations of  $R_{23} = R_{31} = R$ .

For three particles lying in the  $x$ - $y$  plane as shown in Fig. 1, the corresponding zeroth-order wave functions are

$$\Psi_{1,\perp}^{(0)} = \frac{1}{\sqrt{2}}[|n_0 1; n_0 0; n'_0 0\rangle + |n_0 0; n_0 1; n'_0 0\rangle], \quad (68)$$

TABLE VII. Long-range additive interaction coefficients (in a.u.) of the Li( $2^2S$ )-Li( $2^2P$ )-Li $^+$ ( $2^1S$ ) system for two different types of the zeroth-order wave functions, where the three particles lie collinearly on the  $z$  axis (similar to the  $p1$  orientation of the two-body system shown in Fig. 2). The numbers in parentheses represent the computational uncertainties.

Coefficients	$^{\infty}\text{Li}$		$^7\text{Li}$		$^6\text{Li}$	
	$\Psi_{1,z}^{(0)}$	$\Psi_{2,z}^{(0)}$	$\Psi_{1,z}^{(0)}$	$\Psi_{2,z}^{(0)}$	$\Psi_{1,z}^{(0)}$	$\Psi_{2,z}^{(0)}$
$C_{3,z}^{(12)}(1, M = 0)$	11.000221(2)	-11.000221(2)	11.001853(2)	-11.001853(2)	11.002125(2)	-11.002125(2)
$C_{3,z}^{(23)}(1, M = 0)$	5.4099696(1)	5.4099696(1)	5.4096296(1)	5.4096296(1)	5.4095731(1)	5.4095731(1)
$C_{3,z}^{(31)}(1, M = 0)$	5.4099696(1)	5.4099696(1)	5.4096296(1)	5.4096296(1)	5.4095731(1)	5.4095731(1)
$C_{4,z}^{(23)}(1, M = 0)$	71.9539(4)	71.9539(4)	71.9594(4)	71.9594(4)	71.9604(4)	71.9604(4)
$C_{4,z}^{(31)}(1, M = 0)$	71.9539(4)	71.9539(4)	71.9594(4)	71.9594(4)	71.9604(4)	71.9604(4)
$C_{6,z}^{(12)}(1, M = 0)$	2075.40(3)	2075.40(3)	2076.08(7)	2076.08(7)	2076.19(7)	2076.19(7)
$C_{6,z}^{(23)}(1, M = 0)$	5263.218(3)	5263.218(3)	5263.151(3)	5263.151(3)	5263.140(3)	5263.140(3)
$C_{6,z}^{(31)}(1, M = 0)$	5263.218(3)	5263.218(3)	5263.151(3)	5263.151(3)	5263.140(3)	5263.140(3)
$C_{3,z}^{(12)}(1, M = \pm 1)$	-5.500111(1)	5.500111(1)	-5.500926(1)	5.500926(1)	-5.501062(1)	5.501062(1)
$C_{3,z}^{(23)}(1, M = \pm 1)$	-2.7049847(1)	-2.7049847(1)	-2.7048148(1)	-2.7048148(1)	-2.7047866(1)	-2.7047866(1)
$C_{3,z}^{(31)}(1, M = \pm 1)$	-2.7049847(1)	-2.7049847(1)	-2.7048148(1)	-2.7048148(1)	-2.7047866(1)	-2.7047866(1)
$C_{4,z}^{(23)}(1, M = \pm 1)$	73.1701(4)	73.1701(4)	73.1859(4)	73.1859(4)	73.1885(4)	73.1885(4)
$C_{4,z}^{(31)}(1, M = \pm 1)$	73.1701(4)	73.1701(4)	73.1859(4)	73.1859(4)	73.1885(4)	73.1885(4)
$C_6^{(12)}(1, M = \pm 1)$	1406.68(3)	1406.68(3)	1407.15(5)	1407.15(5)	1407.20(2)	1407.20(2)
$C_{6,z}^{(23)}(1, M = \pm 1)$	-552.8371(7)	-552.8371(7)	-552.8460(5)	-552.8460(5)	-552.8472(7)	-552.8472(7)
$C_{6,z}^{(31)}(1, M = \pm 1)$	-552.8371(7)	-552.8371(7)	-552.8460(5)	-552.8460(5)	-552.8472(7)	-552.8472(7)

$$\Psi_{2,\perp}^{(0)} = \frac{1}{\sqrt{2}}[|n_0 1; n_0 0; n'_0 0\rangle - |n_0 0; n_0 1; n'_0 0\rangle], \quad (69)$$

where the symbol  $\perp$  indicates specificity to the  $x$ - $y$  planar configuration with  $R_{23} = R_{31} = R$ . Note that Eqs. (68) and (69) include the special case of the three particles lying collinearly on the  $x$  axis, i.e., the orientation  $p3$ .

### B. Additive coefficients: Evaluation

Using the degenerate perturbation theory, we find that different from the ground-state Li $_3^+$  trimer (where there is no analogous quantum three-body effect for these long-range additive coefficients [12]), the atomic states  $a$  and  $b$  and the corresponding additive coefficients are changing with

TABLE VIII. Long-range additive interaction coefficients (in a.u.) of the Li( $2^2S$ )-Li( $2^2P$ )-Li $^+$ ( $2^1S$ ) system for two different types of the zeroth-order wave functions, where the three particles lie in the  $x$ - $y$  plane with  $R_{23} = R_{31} = R$  as shown in Fig. 1. Note that this includes the special case of the three particles collinear on the  $x$  axis. The numbers in parentheses represent the computational uncertainties.

Coefficients	$^{\infty}\text{Li}$		$^7\text{Li}$		$^6\text{Li}$	
	$\Psi_{1,\perp}^{(0)}$	$\Psi_{2,\perp}^{(0)}$	$\Psi_{1,\perp}^{(0)}$	$\Psi_{2,\perp}^{(0)}$	$\Psi_{1,\perp}^{(0)}$	$\Psi_{2,\perp}^{(0)}$
$C_3^{(12)}(1, M = 0)$	-5.500111(1)	5.500111(1)	-5.500926(1)	5.500926(1)	-5.501062(1)	5.501062(1)
$C_3^{(23)}(1, M = 0)$	-2.7049847(1)	-2.7049847(1)	-2.7048148(1)	-2.7048148(1)	-2.7047866(1)	-2.7047866(1)
$C_3^{(31)}(1, M = 0)$	-2.7049847(1)	-2.7049847(1)	-2.7048148(1)	-2.7048148(1)	-2.7047866(1)	-2.7047866(1)
$C_4^{(23)}(1, M = 0)$	73.1701(4)	73.1701(4)	73.1859(4)	73.1859(4)	73.1885(4)	73.1885(4)
$C_4^{(31)}(1, M = 0)$	73.1701(4)	73.1701(4)	73.1859(4)	73.1859(4)	73.1885(4)	73.1885(4)
$C_6^{(12)}(1, M = 0)$	1406.68(3)	1406.68(3)	1407.15(5)	1407.15(5)	1407.20(2)	1407.20(2)
$C_6^{(23)}(1, M = 0)$	-552.8371(7)	-552.8371(7)	-552.8460(5)	-552.8460(5)	-552.8472(7)	-552.8472(7)
$C_6^{(31)}(1, M = 0)$	-552.8371(7)	-552.8371(7)	-552.8460(5)	-552.8460(5)	-552.8472(7)	-552.8472(7)
$C_3^{(12)}(1, M = \pm 1)$	2.750054(1)	-2.750054(1)	2.750462(1)	-2.750462(1)	2.750530(1)	-2.750530(1)
$C_3^{(23)}(1, M = \pm 1)$	1.3524924(1)	1.3524924(1)	1.3524074(1)	1.3524074(1)	1.3523932(1)	1.3523932(1)
$C_3^{(31)}(1, M = \pm 1)$	1.3524924(1)	1.3524924(1)	1.3524074(1)	1.3524074(1)	1.3523932(1)	1.3523932(1)
$C_4^{(23)}(1, M = \pm 1)$	72.5620(5)	72.5620(5)	72.5727(5)	72.5727(5)	72.5745(5)	72.5745(5)
$C_4^{(31)}(1, M = \pm 1)$	72.5620(5)	72.5620(5)	72.5727(5)	72.5727(5)	72.5745(5)	72.5745(5)
$C_6^{(12)}(1, M = \pm 1)$	1741.06(5)	1741.06(5)	1741.59(4)	1741.59(4)	1741.68(4)	1741.68(4)
$C_6^{(23)}(1, M = \pm 1)$	2355.190(2)	2355.190(2)	2355.152(2)	2355.152(2)	2355.146(2)	2355.146(2)
$C_6^{(31)}(1, M = \pm 1)$	2355.190(2)	2355.190(2)	2355.152(2)	2355.152(2)	2355.146(2)	2355.146(2)

TABLE IX. Long-range nonadditive interaction coefficients (in a.u.) of the  $\text{Li}(2^2S)\text{-Li}(2^2P)\text{-Li}^+(2^1S)$  system for two different types of the zeroth-order wave functions, where the three particles form an equally spaced collinear configuration with the ion in the middle lying on the  $x$  axis. The numbers in parentheses represent the computational uncertainties.

Coefficients	$^{\infty}\text{Li}$		$^7\text{Li}$		$^6\text{Li}$	
	$\Psi_{1,\perp}^{(0)}$	$\Psi_{2,\perp}^{(0)}$	$\Psi_{1,\perp}^{(0)}$	$\Psi_{2,\perp}^{(0)}$	$\Psi_{1,\perp}^{(0)}$	$\Psi_{2,\perp}^{(0)}$
$C_{4,2}^{(12,23)}(1, M=0)$	-1873.904(5)	3205.671(5)	-1874.274(5)	3206.351(5)	-1874.334(6)	3206.464(5)
$C_{2,4}^{(31,12)}(1, M=0)$	-1873.904(5)	3205.671(5)	-1874.274(5)	3206.351(5)	-1874.334(6)	3206.464(5)
$C_{3,3}^{(12,23)}(1, M=0)$	244.58680(3)	-244.58680(3)	244.65297(5)	-244.65297(5)	244.66399(5)	-244.66399(5)
$C_{3,3}^{(23,31)}(1, M=0)$	1.0592047(2)	-1.0592047(2)	1.0597875(3)	-1.0597875(3)	1.0598847(2)	-1.0598847(2)
$C_{3,3}^{(31,12)}(1, M=0)$	244.58680(3)	-244.58680(3)	244.65297(5)	-244.65297(5)	244.66399(5)	-244.66399(5)
$C_{4,2}^{(12,23)}(1, M=\pm 1)$	936.951(3)	-1602.836(3)	937.136(3)	-1603.176(3)	937.167(3)	-1603.231(2)
$C_{2,4}^{(31,12)}(1, M=\pm 1)$	936.951(3)	-1602.836(3)	937.136(3)	-1603.176(3)	937.167(3)	-1603.231(2)
$C_{3,3}^{(12,23)}(1, M=\pm 1)$	611.46703(6)	-611.46703(6)	611.6324(1)	-611.6324(1)	611.6600(1)	-611.6600(1)
$C_{3,3}^{(23,31)}(1, M=\pm 1)$	2.6480119(5)	-2.6480119(5)	2.649468(1)	-2.649468(1)	2.6497127(6)	-2.6497127(6)
$C_{3,3}^{(31,12)}(1, M=\pm 1)$	611.46703(6)	-611.46703(6)	611.6324(1)	-611.6324(1)	611.6600(1)	-611.6600(1)

different geometries of the three-body system for the excited  $\text{Li}_3^+$  trimer. This phenomenon is absolutely a kind of quantum three-body effect, which is caused by the degeneracy of the excited  $\text{Li}_3^+$  trimer. In contrast, for the specific geometries with  $R_{23} = R_{31} = R$ , we find that the atomic states and the corresponding additive interaction coefficients would remain unchanged due to the symmetry of the three-body system. This feature makes these coefficients useful in the quantum-chemistry studies. In the present paper we give the calculations of the long-range coefficients for these specific configurations. The additive coefficients  $C_n^{(IJ)}$  [to be in Eqs. (17) and (21)] are calculated for the specific three-body  $\text{Li}(2^2S)\text{-Li}(2^2P)\text{-Li}^+(1^1S)$  system lying on the  $z$  axis or in the  $x$ - $y$  plane. The numerical values are shown in Tables VII and VIII, where we can also find the orientation dependence (which is demonstrated in Sec. IIH for the two-body system) of the long-range interaction coefficients for the excited  $\text{Li}_3^+$  trimer.

For the numerical values of these additive coefficients, we note that the leading long-range interaction coefficient between two neutral atoms  $C_3^{(12)}(1, M)$  can be positive (attractive) or negative (repulsive), corresponding to the different atomic states related to the symmetry of the system. The leading terms  $C_{3,z}^{(23)}(1, M=\pm 1)$  and  $C_{3,z}^{(31)}(1, M=\pm 1)$  (see Table VII) and  $C_3^{(23)}(1, M=0)$  and  $C_3^{(31)}(1, M=0)$  (see Table VIII) are always negative, which represents the repulsive interactions between the charge of the  $\text{Li}^+(1^1S)$  ion and the permanent electric quadrupole moments of the  $\text{Li}(2^2P)$  atom generated by its anisotropic charge distribution along the  $z$  axis for  $M=\pm 1$  and  $M=0$  states, respectively. The leading terms  $C_{3,z}^{(23)}(1, M=0)$  and  $C_{3,z}^{(31)}(1, M=0)$  (see Table VII) and  $C_3^{(23)}(1, M=\pm 1)$  and  $C_3^{(31)}(1, M=\pm 1)$  (see Table VIII) are always positive (attractive), which is caused by the induction effect of the  $\text{Li}^+(1^1S)$  atom. Similarly, the inductive terms  $C_{4,z}^{(23)}(1, M)$  and  $C_{4,z}^{(31)}(1, M)$  (see Table VII) and  $C_4^{(23)}(1, M)$  and  $C_4^{(31)}(1, M)$  (see Table VIII) are also always positive (attractive). Their numerical values are the linear combinations of the inductive interactions of the  $\text{Li}(2^2S)\text{-Li}^+(1^1S)$  system and the  $\text{Li}(2^2P)\text{-Li}^+(1^1S)$  system

[Eqs. (46) and (47)]. The  $C_{6,z}^{(23)}(1, M)$  and  $C_{6,z}^{(31)}(1, M)$  (see Table VII) and  $C_6^{(23)}(1, M)$  and  $C_6^{(31)}(1, M)$  (see Table VIII) are also the linear combinations of inductive and dispersion interactions of the  $\text{Li}(2^2S)\text{-Li}^+(1^1S)$  system and the  $\text{Li}(2^2P)\text{-Li}^+(1^1S)$  system [Eqs. (49) and (50)].

### C. Nonadditive coefficients: Collinear and equilateral triangle

The nonadditive interaction coefficients of Eq. (33) show a dependence on the interior angles of the three-body system. It is not practical to calculate the nonadditive coefficients for arbitrary cases when  $R_{23} = R_{31} = R$ . However, for the collinear and the equilateral triangle configuration, which fortunately are probably the most interesting configurations, we can evaluate specific values. In this section, these coefficients are given for two geometries: an equally spaced collinear configuration with the ion in the center ( $R_{23} = R_{31} = R$ ) (see Table IX) and an equilateral triangle configuration ( $R_{23} = R_{31} = R_{12} = R$ ) (see Table X). Different from the ground-state  $\text{Li}_3^+$  trimer demonstrated in Ref. [12], the long-range nonadditive interactions of the current excited  $\text{Li}_3^+$  trimer appear in the second-order correction, not in the third-order correction. This phenomenon is caused by the degeneracy of the three-body system introduced by the presence of the excited  $\text{Li}(2^2P)$  atom. From Tables IX and X we can find that most of the nonadditive coefficients are indeed different from each other for these two geometries, even with the same atomic states as shown in Eqs. (68) and (69). This kind of three-body effect is caused by the different interior angles of the two geometries associated with the magnetic quantum number  $M$  of the  $\text{Li}(2^2P)$  atom, which can also be easily figured out from Eqs. (34)–(38). Also, for the different interior angles of the geometries and for the different magnetic quantum number  $M$ , these nonadditive terms can be attractive or repulsive.

Due to the induction effect of the  $\text{Li}^+(1^1S)$  cation, some of these nonadditive coefficients are enhanced. For example, from Table IX we find that the inductive nonadditive coefficients  $|C_{4,2}^{(12,23)}(1, M=0)| = |C_{2,4}^{(31,12)}(1, M=0)| = 1873.904(5)$  a.u. are much larger than the dispersion

TABLE X. Long-range nonadditive interaction coefficients (in a.u.) of the  $\text{Li}(2^2S)\text{-Li}(2^2P)\text{-Li}^+(2^1S)$  system for two different types of the zeroth-order wave functions, where the three particles form an equilateral triangle. The numbers in parentheses represent the computational uncertainties.

Coefficients	$^{\infty}\text{Li}$		$^7\text{Li}$		$^6\text{Li}$	
	$\Psi_{1,\perp}^{(0)}$	$\Psi_{2,\perp}^{(0)}$	$\Psi_{1,\perp}^{(0)}$	$\Psi_{2,\perp}^{(0)}$	$\Psi_{1,\perp}^{(0)}$	$\Psi_{2,\perp}^{(0)}$
$C_{4,2}^{(12,23)}(1, M = 0)$	-936.951(3)	1602.836(3)	-937.136(3)	1603.176(3)	-937.167(3)	1603.231(2)
$C_{2,4}^{(31,12)}(1, M = 0)$	-936.951(3)	1602.836(3)	-937.136(3)	1603.176(3)	-937.167(3)	1603.231(2)
$C_{3,3}^{(12,23)}(1, M = 0)$	244.58680(3)	-244.58680(3)	244.65297(5)	-244.65297(5)	244.66399(5)	-244.66399(5)
$C_{3,3}^{(23,31)}(1, M = 0)$	1.0592047(2)	-1.0592047(2)	1.0597875(3)	-1.0597875(3)	1.0598847(2)	-1.0598847(2)
$C_{3,3}^{(31,12)}(1, M = 0)$	244.58680(3)	-244.58680(3)	244.65297(5)	-244.65297(5)	244.66399(5)	-244.66399(5)
$C_{4,2}^{(12,23)}(1, M = \pm 1)$	468.476(1)	-801.417(1)	468.567(2)	-801.587(1)	468.584(1)	-801.616(2)
$C_{2,4}^{(31,12)}(1, M = \pm 1)$	468.476(1)	-801.417(1)	468.567(2)	-801.587(1)	468.584(1)	-801.616(2)
$C_{3,3}^{(12,23)}(1, M = \pm 1)$	-214.01346(2)	214.01346(2)	-214.07137(3)	214.07137(3)	-214.08101(3)	214.08101(3)
$C_{3,3}^{(23,31)}(1, M = \pm 1)$	-0.9268041(2)	0.9268041(2)	-0.9273142(2)	0.9273142(2)	-0.9273991(2)	0.9273991(2)
$C_{3,3}^{(31,12)}(1, M = \pm 1)$	-214.01346(2)	214.01346(2)	-214.07137(3)	214.07137(3)	-214.08101(3)	214.08101(3)

nonadditive one [ $|C_{3,3}^{(23,31)}(1, M = 0)| = 1.059\,204\,7(2)$  a.u. from Table IX] and are even larger than some of the additive dispersion [ $|C_6^{(12)}(1, M = 0)| = 1406.68(3)$  a.u. from Table VIII] and additive inductive ones [ $|C_6^{(23)}(1, M = 0)| = 552.8371(7)$  a.u. from Table VIII] at the same order. The competition between the additive attractive and nonadditive repulsive terms of  $C_6$  for particular geometries will also be discussed in the following section. These large nonadditive inductive interactions would be indispensable in constructing potential surfaces and be very useful in studies of quantum three-body effect for the excited  $\text{Li}_3^+$  trimers.

**D. Long-range potentials: Results**

Evaluating the additive and nonadditive long-range potentials using the coefficients given in Tables VII–X, the potential functions are displayed for two geometries: an equally spaced collinear configuration with  $R_{23} = R_{31} = R$  (see Figs. 4 and 5) and an equilateral triangle with sides of length  $R$  (see Fig. 6). We should indicate that the nonadditive interactions of the

present paper are all evaluated for the geometries lying on the  $x$ - $y$  plane as shown in Fig. 1. Thus, for the three particles lying on the  $z$  axis, only the additive potentials are shown in Fig. 4 with respect to the two-body  $p_1$  situation (see Fig. 2). For the collinear configuration lying on the  $x$ - $y$  plane, the total additive and nonadditive potentials are displayed in Fig. 5. The separations between the  $M = 0$  and  $M = \pm 1$  states are mainly caused by the leading repulsive or attractive electrostatic interaction involving  $C_3$  between the ion and the excited atom. In Fig. 6 we display the total long-range potentials (additive and nonadditive) for the geometry of equilateral triangle lying on the  $x$ - $y$  plane, where a barrier of about  $115\text{ cm}^{-1}$  at internuclear distance of  $17a_0$  is found for the  $\Psi_{1,\perp}^{(0)}(1, M = 0)$  state. The barrier results from the interplay of the repulsive leading terms involving  $C_3$  and the attractive induction interaction involving  $C_4$ . For the other states, the long-range potentials are attractive at all internuclear distances. Note that the data presented in this section do not include exchange energies,

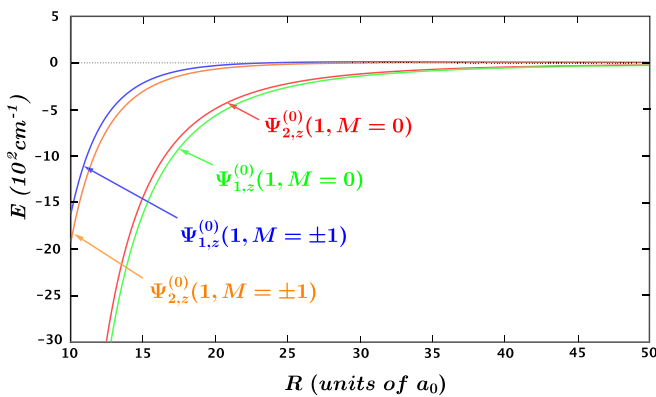


FIG. 4. Long-range additive interaction potentials (in a.u.) of the  $^{\infty}\text{Li}(2^2S)\text{-}^{\infty}\text{Li}(2^2P)\text{-}^{\infty}\text{Li}^+(1^1S)$  system for two types of the zeroth-order wave functions, where three particles lie collinearly on the  $z$  axis. For each curve labeled by a wave function, the plotted curve is the sum of  $\Delta E^{(1)}$  and  $\Delta E^{(2)}$ .

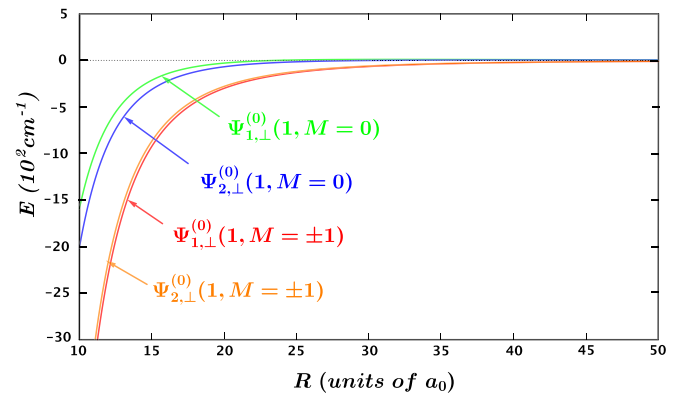


FIG. 5. Long-range interaction potentials (in a.u.) of the  $^{\infty}\text{Li}(2^2S)\text{-}^{\infty}\text{Li}(2^2P)\text{-}^{\infty}\text{Li}^+(1^1S)$  system for two types of the zeroth-order wave functions, where three particles lie collinearly on the  $x$  axis. The plotted potentials include all electrostatic-, dispersion-, and induction-type interactions (additive and nonadditive) up to  $O(R^{-6})$ . For each curve labeled by a wave function, the plotted curve is the sum of  $\Delta E^{(1)}$  and  $\Delta E^{(2)}$ .

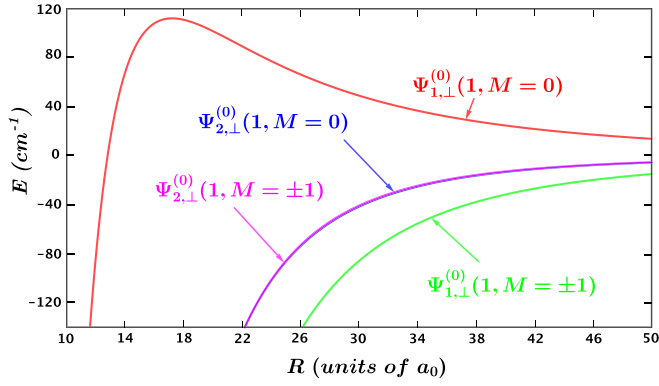


FIG. 6. Long-range interaction potentials (in a.u.) of the  ${}^{\infty}\text{Li}(2^2S)\text{-}{}^{\infty}\text{Li}(2^2P)\text{-}{}^{\infty}\text{Li}^+(1^1S)$  system for two types of the zeroth-order wave functions, where three particles form an equilateral triangle on the  $x$ - $y$  plane. The plotted potentials include all electrostatic-, dispersion-, and induction-type interactions (additive and nonadditive) up to  $O(R^{-6})$ . For each curve labeled by a wave function, the plotted curve is the sum of  $\Delta E^{(1)}$  and  $\Delta E^{(2)}$ .

which may contribute at these internuclear distances. We will discuss their contributions in the following section.

### E. Strong nonadditive potentials and switching off the additive potentials

As we discussed before, the nonadditive collective effect of the three-body system is caused by its degeneracy, which is introduced by the presence of the excited  $\text{Li}(2^2P)$  atom.

Meanwhile, the presence of the  $\text{Li}^+(1^1S)$  ion introduces the induction effect, which strongly enhances the nonadditive (collective) interaction, as demonstrated in Sec. III C. In this section we present a graphical comparison of the additive and nonadditive potentials for the equilateral triangle and collinear ( $R_{23} = R_{31} = R$ ) configurations (see Fig. 7).

The figure illustrates that the nonadditive potentials are significant and can even be stronger than the net contribution from the additive potentials. For example, for the equilateral triangle configuration, the magnitude of the additive contribution [Fig. 7(a)] becomes less than the nonadditive contribution [Fig. 7(b)] around  $R \sim 14a_0$ . Indeed, we find that there are specific internuclear distances at which the additive contributions sum to zero, leaving only nonadditive contributions. Denoting these special distances by  $\bar{R}$ , for the equilateral triangle configuration, the additive cancellation occurs at  $\bar{R} = 13.58a_0$  for the  $\Psi_{1,\perp}(1, M = 0)$  state with a net energy of  $48.42 \text{ cm}^{-1}$ . For the collinear configuration the additive cancellation occurs at  $\bar{R} = 23.68a_0$  for the  $\Psi_{1,\perp}(1, M = 0)$  state with a net energy of  $0.25 \text{ cm}^{-1}$  and at  $\bar{R} = 30.69a_0$  for the  $\Psi_{2,\perp}(1, M = 0)$  state with a net energy of  $-0.09 \text{ cm}^{-1}$ .

We now, as promised in Sec. I C, draw a comparison with trapped cold polar molecules. When the additive (two-body) contributions sum to zero at a distance  $\bar{R}$ , Eq. (16) reduces to

$$\Delta E(\bar{R}) = \Delta E_{\text{non}}^{(2)}(\bar{R}). \quad (70)$$

Comparing Eq. (33) for  $\Delta E_{\text{non}}^{(2)}$  with Eq. (2) for the three-body lattice interaction, we observe that they are precisely the same form. Since our results are specific to three particles, the collinear case is most similar to the case of trapped polar

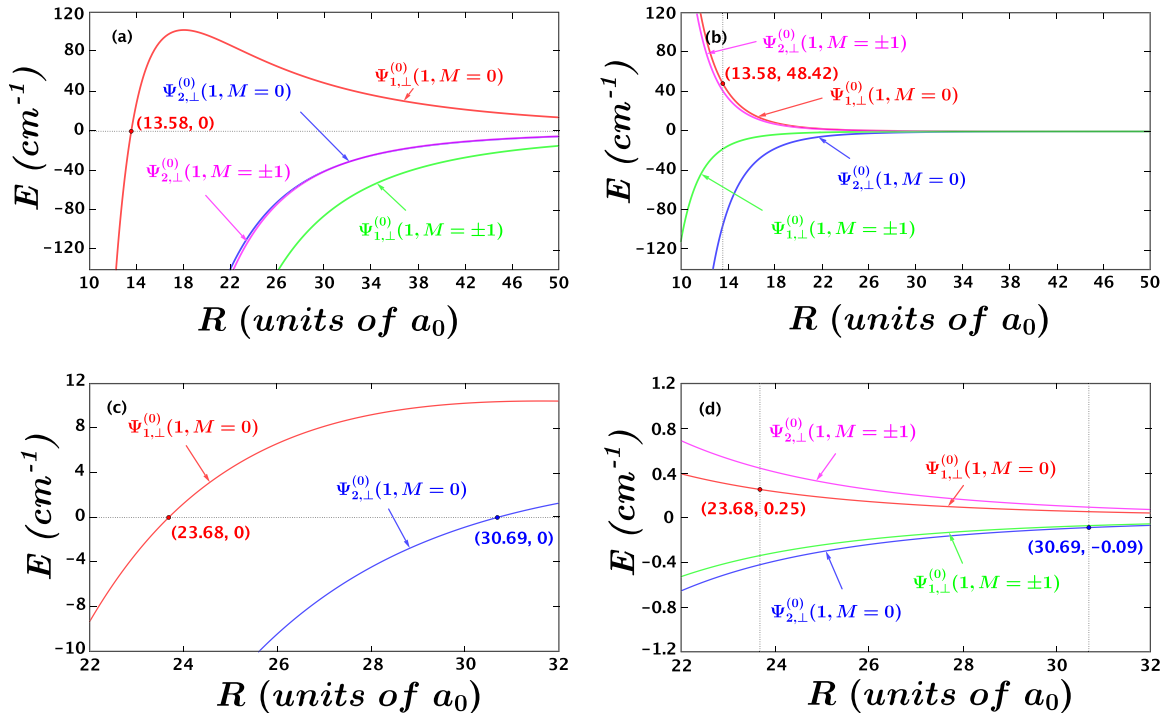


FIG. 7. Comparison of long-range (a) and (c) additive potentials and (b) and (d) nonadditive (collective) potentials (in a.u.) of the  ${}^{\infty}\text{Li}(2^2S)\text{-}{}^{\infty}\text{Li}(2^2P)\text{-}{}^{\infty}\text{Li}^+(1^1S)$  system for two types of the zeroth-order wave functions with  $R_{23} = R_{31} = R$ : (a) and (b) equilateral triangle and (c) and (d) equally spaced collinear configurations. At the labeled points, the two-body additive potentials sum to zero, leaving only the net nonadditive collective potentials.

molecules in a linear configuration, such as shown in Fig. 1(a) of Ref. [64]. Our intriguing result deserves further study. In retrospect, we can understand the appearance of a cancellation analogous to that found for trapped polar molecules: The anisotropy of the present system due to the  $\text{Li}(2^2P)$  atom in the presence of the  $\text{Li}^+(1^1S)$  ion charge is physically similar to the dipole-dipole interaction in the presence of an external electric field in the optical lattice case. To gauge precisely the physical potential energies at the special distances  $\bar{R}$ , treatment of the exchange energy contributions, or equivalently quantum-chemical calculations, would be desirable. However, by analogy with the  $\text{Li}^+(1^1S)\text{-Li}(2^2P)$  results that we presented in Sec. III, we observe that the values of  $\bar{R}$  are probably sufficiently large so that it is likely that only exchange energies will contribute. Nevertheless, the present result suggests an intriguing similarity between the  $\text{Li}(2^2S)\text{-Li}(2^2P)\text{-Li}^+(1^1S)$  system and the trapped cold polar molecule scenario.

#### IV. CONCLUSION

The long-range additive and nonadditive interaction potentials for the  $\text{Li}(2^2S)\text{-Li}(2^2P)\text{-Li}^+(1^1S)$  system were calculated by using degenerate perturbation theory. We found that all the first-order and second-order additive and non-additive interaction coefficients show a dependence on the geometrical configurations of the system. The nonadditive interactions depend on both the atomic states and the interior angles of the configurations. The degeneracy of the system caused by the presence of the  $\text{Li}(2^2P)$  atom leads to the three-body collective effect. The presence of the  $\text{Li}^+(1^1S)$  ion was found to enhance this collective effect, which makes the

three-body nonadditive collective interactions of the system even stronger than the two-body additive interactions for some specific configurations of the three-body system. For the two particular configurations with  $R_{23} = R_{31} = R$ , the equilateral triangle configuration and the equally spaced collinear configuration, the interaction coefficients were evaluated with highly accurate wave functions calculated variationally in Hylleraas coordinates. In addition, for the  $\text{Li}(2^2S)\text{-Li}(2^2P)\text{-Li}^+(1^1S)$  system, the two-body additive interaction can be switched off, leaving only three-body nonadditive interactions for particular geometries, which makes this three-body system a prospective platform to study the quantum collective effect. We demonstrated how two-body interaction potentials can be extracted from our results and gave explicit expressions for the long-range potentials of the  $\text{Li}^+(1^1S)\text{-Li}(2^2P)$  system. The present high-precision results can serve as benchmarks for future quantum-chemical calculations and may be of interest for constructing precise potential energy surfaces. The general formulas for  $A(n_0S)\text{-}A(n'_0L)\text{-}A^{Q+}(n''_0S)$  are listed in the Supplemental Material.

#### ACKNOWLEDGMENTS

This work was supported by NSERC of Canada and by the Strategic Priority Research Program of the Chinese Academy of Sciences under Grant No. XDB21030300. J.F.B. was supported in part by the U.S. NSF through Grant No. PHY-1521560 for the Institute of Theoretical Atomic, Molecular, and Optical Physics at Harvard University and Smithsonian Astrophysical Observatory.

- 
- [1] M. Tomza, K. Jachymski, R. Gerritsma, A. Negretti, T. Calarco, Z. Idziaszek, and P. S. Julienne, *Rev. Mod. Phys.* **91**, 035001 (2019).
- [2] M. Lepers, O. Dulieu, and V. Kokoouline, *Phys. Rev. A* **82**, 042711 (2010).
- [3] M. Lepers, R. Vexiau, N. Bouloufa, O. Dulieu, and V. Kokoouline, *Phys. Rev. A* **83**, 042707 (2011).
- [4] J. Pérez-Ríos, M. Lepers, and O. Dulieu, *Phys. Rev. Lett.* **115**, 073201 (2015).
- [5] M. Śmiałkowski and M. Tomza, *Phys. Rev. A* **101**, 012501 (2020).
- [6] D. Cano and J. Fortágh, *Phys. Rev. A* **86**, 043422 (2012).
- [7] J. Qian, *J. Opt. Soc. Am. B* **33**, 1749 (2016).
- [8] M. A. Baranov, M. Dalmonte, G. Pupillo, and P. Zoller, *Chem. Rev.* **112**, 5012 (2012).
- [9] M. Kiffner, W. Li, and D. Jaksch, *Phys. Rev. Lett.* **111**, 233003 (2013).
- [10] P.-G. Yan, L.-Y. Tang, Z.-C. Yan, and J. F. Babb, *Phys. Rev. A* **94**, 022705 (2016).
- [11] P.-G. Yan, L.-Y. Tang, Z.-C. Yan, and J. F. Babb, *Phys. Rev. A* **97**, 042710 (2018).
- [12] P.-G. Yan, L.-Y. Tang, Z.-C. Yan, and J. F. Babb, *Phys. Rev. A* **101**, 032702 (2020).
- [13] R. J. Bell, *J. Phys. B* **3**, L101 (1970).
- [14] B. M. Axilrod and E. Teller, *J. Chem. Phys.* **11**, 299 (1943).
- [15] P. Xu, M. Alkan, and M. S. Gordon, *Chem. Rev.* **120**, 12343 (2020).
- [16] V. F. Lotrich and K. Szalewicz, *Phys. Rev. Lett.* **79**, 1301 (1997).
- [17] V. F. Lotrich and K. Szalewicz, *J. Chem. Phys.* **106**, 9668 (1997).
- [18] V. F. Lotrich and K. Szalewicz, *J. Chem. Phys.* **112**, 112 (2000).
- [19] E. M. Mas, V. F. Lotrich, and K. Szalewicz, *J. Chem. Phys.* **110**, 6694 (1999).
- [20] J. Hecht and R. Brookfield, *New Scientist* **92**, 224 (1981).
- [21] D. R. Herschbach, in *Proceedings of the Conference on Potential Energy Surfaces in Chemistry*, edited by W. A. Lester, Jr. (IBM Research Laboratory, San Jose, 1971), pp. 44–55.
- [22] B. Gao, [arXiv:2008.08018](https://arxiv.org/abs/2008.08018).
- [23] C. A. Mead and D. G. Truhlar, *J. Chem. Phys.* **70**, 2284 (1979); **78**, 6344E (1983).
- [24] M. Baer, *Beyond Born-Oppenheimer: Conical Intersections and Electronic Nonadiabatic Coupling Terms* (Wiley, Hoboken, 2006).
- [25] C. Jungen and A. J. Merer, *Mol. Phys.* **40**, 1 (1980).
- [26] J. Macek, *Z. Phys. D* **3**, 31 (1986).
- [27] J. H. Macek, *Phys. Scr.* **76**, C3 (2007).
- [28] B. Paredes, T. Keilmann, and J. I. Cirac, *Phys. Rev. A* **75**, 053611 (2007).
- [29] M. Tizniti, S. D. Le Picard, F. Lique, C. Berteloite, A. Canosa, M. H. Alexander, and I. R. Sims, *Nat. Chem.* **6**, 141 (2014).
- [30] T. de Jongh, M. Besemer, Q. Shuai, T. Karman, A. van der Avoird, G. C. Groenenboom, and S. Y. T. van de Meerakker, *Science* **368**, 626 (2020).

- [31] A. J. Daley, J. M. Taylor, S. Diehl, M. Baranov, and P. Zoller, *Phys. Rev. Lett.* **102**, 040402 (2009); **102**, 179902E (2009).
- [32] T. Kraemer, M. Mark, P. Waldburger, J. G. Danzl, C. Chin, B. Engeser, A. D. Lange, K. Pilch, A. Jaakkola, H.-C. Nägerl, and R. Grimm, *Nature (London)* **440**, 315 (2006).
- [33] U. Eismann, L. Khaykovich, S. Laurent, I. Ferrier-Barbut, B. S. Rem, A. T. Grier, M. Delehaye, F. Chevy, C. Salomon, L.-C. Ha, and C. Chin, *Phys. Rev. X* **6**, 021025 (2016).
- [34] G. Guillon, M. Lepers, and P. Honvault, *Phys. Rev. A* **102**, 012810 (2020).
- [35] T. F. Giesen, B. Mookerjee, G. W. Fuchs, A. A. Breier, D. Witsch, R. Simon, and J. Stutzki, *Astron. Astrophys.* **633**, A120 (2020).
- [36] K. Matsumura, H. Kanamori, K. Kawaguchi, and E. Hirota, *J. Chem. Phys.* **89**, 3491 (1988).
- [37] Y. Xie, H. Zhao, Y. Wang, Y. Huang, T. Wang, X. Xu, C. Xiao, Z. Sun, D. H. Zhang, and X. Yang, *Science* **368**, 767 (2020).
- [38] S. Lepp, V. Buch, and A. Dalgarno, *Astrophys. J. Supl. Ser.* **98**, 345 (1995).
- [39] S. Lepp, P. C. Stancil, and A. Dalgarno, *J. Phys. B* **35**, R57 (2002).
- [40] C. M. R. Rocha and A. J. C. Varandas, *J. Phys. Chem. A* **123**, 8154 (2019).
- [41] M. Lepers, B. Bussery-Honvault, and O. Dulieu, *J. Chem. Phys.* **137**, 234305 (2012).
- [42] M. Ayouz and D. Babikov, *J. Chem. Phys.* **138**, 164311 (2013).
- [43] Z. Varga, Y. Paukku, and D. G. Truhlar, *J. Chem. Phys.* **147**, 154312 (2017).
- [44] A. I. Boothroyd, W. J. Keogh, P. G. Martin, and M. R. Peterson, *J. Chem. Phys.* **104**, 7139 (1996).
- [45] A. J. C. Varandas, in *Advances in Chemical Physics*, edited by I. Prigogine and S. A. Rice (Wiley, New York, 1988), Vol. 74, pp. 255–338.
- [46] A. J. C. Varandas and A. A. C. C. Pais, *J. Chem. Soc. Faraday Trans.* **89**, 1511 (1993).
- [47] J. Ángyán, J. Dobson, G. Jansen, and T. Gould, *London Dispersion Forces in Molecules, Solids and Nano-structures: An Introduction to Physical Models and Computational Methods* (Royal Society of Chemistry, Cambridge, 2020).
- [48] C. Berteloite, M. Lara, A. Bergeat, S. D. Le Picard, F. Dayou, K. M. Hickson, A. Canosa, C. Naulin, J.-M. Launay, I. R. Sims, and M. Costes, *Phys. Rev. Lett.* **105**, 203201 (2010).
- [49] M. Lepers and O. Dulieu, *Phys. Chem. Chem. Phys.* **13**, 19106 (2011).
- [50] V. Olaya, J. Pérez-Ríos, and F. Herrera, *Phys. Rev. A* **101**, 032705 (2020).
- [51] S. Willitsch, in *Advances in Chemical Physics*, edited by S. A. Rice and A. R. Dinner (Wiley, Hoboken, 2017), Vol. 162, pp. 307–340.
- [52] P. Puri, M. Mills, C. Schneider, I. Simbotin, J. A. Montgomery, R. Côté, A. G. Suits, and E. R. Hudson, *Science* **357**, 1370 (2017).
- [53] A. D. Dörfler, E. Yurtsever, P. Villarreal, T. González-Lezana, F. A. Gianturco, and S. Willitsch, *Phys. Rev. A* **101**, 012706 (2020).
- [54] S. Magnier, S. Rousseau, A. Allouche, G. Hadinger, and M. Aubert-Frécon, *Chem. Phys.* **246**, 57 (1999).
- [55] D. Rabli and R. McCarroll, *Chem. Phys.* **487**, 23 (2017).
- [56] P. Jasik, J. Wilczyński, and J. E. Sienkiewicz, *Eur. Phys. J. Spec. Top.* **144**, 85 (2007).
- [57] S. J. Dunne, D. J. Searles, and E. I. von Nagy-Felsobuki, *Spectrochim. Acta A* **43**, 699 (1987).
- [58] D. J. Searles, S. J. Dunne, and E. I. von Nagy-Felsobuki, *Spectrochim. Acta A* **44**, 505 (1988).
- [59] D. J. Searles, S. J. Dunne, and E. I. von Nagy-Felsobuki, *Spectrochim. Acta A* **44**, 985 (1988).
- [60] D. J. Searles and E. I. von Nagy-Felsobuki, *J. Chem. Phys.* **95**, 1107 (1991).
- [61] J. R. Henderson, S. Miller, and J. Tennyson, *Spectrochim. Acta A* **44**, 1287 (1988).
- [62] F. Wang and E. I. von Nagy-Felsobuki, *Spectrochim. Acta A* **51**, 1827 (1995).
- [63] I. Tamásy-Lentei and J. Szaniszló, *J. Mol. Struct. THEOCHEM* **501–502**, 403 (2000).
- [64] H. P. Büchler, A. Micheli, and P. Zoller, *Nat. Phys.* **3**, 726 (2007).
- [65] K. K. Ni, S. Ospelkaus, D. Wang, G. Quémener, B. Neyenhuis, M. H. G. de Miranda, J. L. Bohn, J. Ye, and D. S. Jin, *Nature (London)* **464**, 1324 (2010).
- [66] A. Klein, Y. Shagam, W. Skomorowski, P. S. Żuchowski, M. Pawlak, L. M. C. Janssen, N. Moiseyev, S. Y. T. van de Meerakker, A. van der Avoird, C. P. Koch, and E. Narevicius, *Nat. Phys.* **13**, 35 (2017).
- [67] L. Anderegg, S. Burchesky, Y. Bao, S. S. Yu, T. Karman, E. Chae, K.-K. Ni, W. Ketterle, and J. M. Doyle, [arXiv:2102.04365](https://arxiv.org/abs/2102.04365).
- [68] J.-R. Li, W. G. Tobias, K. Matsuda, C. Miller, G. Valtolina, L. D. Marco, R. R. W. Wang, L. Lassablière, G. Quémener, J. L. Bohn, and J. Ye, [arXiv:2103.06246](https://arxiv.org/abs/2103.06246).
- [69] J. Y. Zhang and Z. C. Yan, *J. Phys. B* **37**, 723 (2004).
- [70] L. Y. Tang, Z. C. Yan, T. Y. Shi, and J. F. Babb, *Phys. Rev. A* **79**, 062712 (2009).
- [71] Z. C. Yan and G. W. F. Drake, *J. Phys. B* **30**, 4723 (1997).
- [72] G. W. F. Drake and Z. C. Yan, *Phys. Rev. A* **52**, 3681 (1995).
- [73] Z. C. Yan and G. W. F. Drake, *Chem. Phys. Lett.* **259**, 96 (1996).
- [74] See Supplemental Material at <http://link.aps.org/supplemental/10.1103/PhysRevA.104.022807> for details of the derivation of perturbation formulas.
- [75] M. Rérat, M. Mérawa, and C. Pouchan, *Phys. Rev. A* **45**, 6263 (1992).
- [76] M. Rérat and C. Pouchan, *Phys. Rev. A* **49**, 829 (1994).
- [77] M. Rérat, B. Bussery, and M. Frécon, *J. Mol. Spectrosc.* **182**, 260 (1997).
- [78] M. Caffarel, M. Rérat, and C. Pouchan, *Phys. Rev. A* **47**, 3704 (1993).
- [79] J. Pipin and D. M. Bishop, *Phys. Rev. A* **47**, R4571 (1993).
- [80] S. Cohen and S. I. Themelis, *J. Phys. B* **38**, 3705 (2005).
- [81] W. R. Johnson, U. I. Safronova, A. Derevianko, and M. S. Safronova, *Phys. Rev. A* **77**, 022510 (2008).
- [82] M. Chibisov and R. Janev, *Phys. Rep.* **166**, 1 (1988).
- [83] K. M. Jones, E. Tiesinga, P. D. Lett, and P. S. Julienne, *Rev. Mod. Phys.* **78**, 483 (2006).